Nonlinear Multiresolution Signal Decomposition Schemes—Part II: Morphological Wavelets

Henk J. A. M. Heijmans, *Member, IEEE*, and John Goutsias, *Senior Member, IEEE*

***Abstract*—In its original form, the wavelet transform is a linear tool. However, it has been increasingly recognized that nonlinear extensions are possible. A major impulse to the development of nonlinear wavelet transforms has been given by the introduction of the lifting scheme by Sweldens. The aim of this paper, which is a sequel of a previous paper devoted exclusively to the pyramid transform, is to present an axiomatic framework encompassing most existing linear and nonlinear wavelet decompositions. Furthermore, it introduces some, thus far unknown, wavelets based on mathematical morphology, such as the morphological Haar wavelet, both in one and two dimensions. A general and flexible approach for the construction of nonlinear (morphological) wavelets is provided by the lifting scheme. This paper briefly discusses one example, the max-lifting scheme, which has the intriguing property that preserves local maxima in a signal over a range of scales, depending on how local or global these maxima are.**

***Index Terms*—Coupled and uncoupled wavelet decomposition, lifting scheme, mathematical morphology, max-lifting, morphological operators, multiresolution signal decomposition, nonlinear wavelet transform.**

I. Introduction

TODAY, it is generally accepted that multiresolution approaches, such as pyramids and wavelets, are important in signal and image processing applications. This is largely due to the fact that signals (and images in particular) often contain physically relevant features at many scales or resolutions. For a proper understanding of such signals, multiresolution (or multiscale) techniques are indispensable. But there exist other good reasons for why taking recourse to multiresolution approaches. A major one is that multiresolution algorithms may offer some attractive computational advantages.

In a previous paper [1], to be referred to here as Part I, we have presented an axiomatic framework for pyramid decompositions of signals, which encompasses several existing approaches; in particular, linear pyramids (such as the Laplacian pyramid proposed by Burt and Adelson [2]), and morphological tools such as the skeleton [3]. A short overview of this framework is provided in Section II.

Wavelet signal decomposition is a relatively new tool developed over the past ten or fifteen years. It has attracted the interest of scientists from various disciplines, in particular mathematics, physics, computer science, and electrical engineering. Although wavelet decomposition is a *linear* signal analysis tool, it is starting to be recognized that nonlinear extensions are possible [4]–[22]. The *lifting scheme*, recently introduced by Sweldens [23]–[25] (see also [26] for a predecessor to this scheme, known as a "ladder network"), has provided a useful way to construct nonlinear wavelet decompositions. The enormous flexibility and freedom that the lifting scheme offers has challenged researchers to develop various nonlinear wavelet transforms [4]–[13], [17], [19], [21], [22], [27].

The literature on nonlinear wavelet decompositions, or *critically decimated nonlinear filter banks* as they are sometimes called, is not extensive. In 1991, Pei and Chen [28], [29] were among the first to propose a nonredundant (in the sense that preserves the number of pixels in the original image) nonlinear subband decomposition scheme based on mathematical morphology. Their approach however does not guarantee perfect reconstruction. In 1994, Egger and Li [4] proposed a nonlinear decomposition scheme with perfect reconstruction based on a median-type operator (see also [6]). Independently, Florêncio and Schafer [5] have presented a similar decomposition; see also [7, Ch. 7]. More recently, Queiroz *et al.* [21] proposed a nonlinear wavelet decomposition, corresponding to the quincunx sampling grid, for low-complexity image coding; see also [7, Ch. 8]. In [7], Florêncio discusses nonlinear perfect reconstruction filter banks in more detail, and attempts to give a better understanding of these issues by relating them to the so-called *critical morphological sampling theorem*. In [9], Cha and Chaparro constructed a nonlinear wavelet decomposition scheme by means of a morphological opening operator. The resulting signal decomposition scheme guarantees perfect reconstruction. However, these authors did not have at their disposal the lifting scheme, which was developed during the same period [23]–[25]. The same remark applies to the work of Hampson and Pesquet [8], [11], [17] who developed nonlinear perfect reconstruction filter banks by considering a triangular form of the polyphase representation of a filter bank. The resulting approach is more or less identical to the lifting scheme.

In four recent papers [10], [12], [13], [22], Claypoole *et al.* use the lifting scheme to build nonlinear wavelet transforms. In the first paper [10], they propose an adaptive lifting step using a nonlinear selection criterion. In the other three papers [12], [13], [22], they use combinations of linear and nonlinear lifting

Manuscript received September 14, 1999; revised June 7, 2000. This work was supported in part by NATO Collaborative Research Grant CRG.971503. J. Goutsias was also supported by the Office of Naval Research, Mathematical, Computer, and Information Sciences Division under ONR Grant N00014-90-1345, and the National Science Foundation under NSF Award 9729576. H. Heijmans was also supported by INTAS under Grant 96-785. The associate editor coordinating the review of this manuscript and approving it for publication was Prof. Pierre Moulin.

H. J. A. M. Heijmans is with the Centre for Mathematics and Computer Science (CWI), 1090 GB Amsterdam, The Netherlands (e-mail: henkh@cwi.nl)

J. Goutsias is with the Center for Imaging Science and the Department of Electrical and Computer Engineering, The Johns Hopkins University, Baltimore, MD 21218 USA (e-mail: goutsias@jhu.edu).

Publisher Item Identifier S 1057-7149(00)09389-1.

steps (based on a median operator), and discuss applications in compression and denoising.

Many of the schemes proposed in the previously mentioned papers are special cases of the general schemes discussed in this paper. Therefore, the theory presented here provides a rather general framework for constructing nonlinear filter banks with perfect reconstruction. It is worth noticing however that the proposed theory depends on three conditions. These conditions are required in order for the proposed multiresolution schemes to guarantee perfect reconstruction and be nonredundant (in the sense that repeated applications of these schemes produce the same result). Moreover, these conditions lead to the concept of nonlinear biorthogonal-like multiresolution analysis, to be discussed in Section III-C, which is a natural extension of the concept of biorthogonal multiresolution analysis associated with linear wavelet decompositions.

The aim of this paper is twofold. First, we present an axiomatic framework to wavelet-type multiresolution signal decomposition that encompasses all known linear and nonlinear wavelet decomposition schemes. Second, we introduce a family of nonlinear wavelets based on morphological operators. The simplest nontrivial example of a morphological wavelet is the so-called morphological Haar wavelet. As we said before, the lifting scheme provides a general method for the construction of various wavelet decompositions. In the linear case, this scheme, in combination with direct methods based on Fourier or z-transform techniques, has lead to a large variation in wavelet decomposition schemes. In the nonlinear case, however, where techniques which are comparable with the (linear) Fourier or z-transform are nonexistent, the lifting scheme is the *only* known general method to construct wavelet decompositions. In this paper, we restrict ourselves to constructions based on morphological operators. Attention is paid to the max-lifting scheme, which has the interesting property that it preserves local maxima of a signal over several scales.

This paper is organized as follows. In Section II, we briefly recall the pyramid transform introduced in Part I. In Section III, we present a general definition of a wavelet transform, which we refer to as the *coupled wavelet decomposition scheme*. A special case is the *uncoupled wavelet decomposition scheme*, a class which the linear biorthogonal wavelets belong to. Section IV is entirely devoted to a simple nontrivial uncoupled wavelet decomposition scheme based on morphological operators, the so-called *morphological Haar wavelet*. We discuss the one-dimensional (1-D) as well as the nonseparable two-dimensional (2-D) case. In Section V, we discuss the lifting scheme within the axiomatic context of this paper. In particular, it is shown that two nonlinear lifting steps generally lead to a coupled wavelet decomposition scheme. A number of examples, based on morphological operators, are discussed. Another important example of the lifting scheme is introduced in Section VI. This is referred to as the *max-lifting scheme*, the most striking property of which is that it preserves local maxima of a signal over several scales, depending on how local or global these maxima are. Finally, in Section VII, we conclude with some final remarks.

II. Pyramid Transform

In Part 1, we presented a comprehensive discussion on the pyramid transform. In this section, we briefly recall the main ideas of that work.

Consider a family V_j of signal spaces. Here, j may range over a finite or an infinite index set. Assume that we have two families of operators, a family $\psi_j^{\uparrow}$ of *analysis operators* mapping V_j into V_{j+1}, and a family $\psi_j^{\downarrow}$ of *synthesis operators* mapping V_{j+1} back into V_j. Here, the upward arrow indicates that the corresponding operator maps a signal to the higher level, whereas the downward arrow indicates that the operator maps a signal to a lower level. The analysis operator $\psi_j^{\uparrow}$ is chosen to reduce information from a signal $x_j \in V_j$, yielding a *scaled signal* $x_{j+1} = \psi_j^{\uparrow}(x_j)$ in V_{j+1}. The synthesis operator $\psi_j^{\downarrow}$ maps the scaled signal x_{j+1} back to $\hat{x}_j = \psi_j^{\downarrow}(x_{j+1})$ in V_j, in such a way that $\psi_j^{\downarrow}\psi_j^{\uparrow}(x_j)$ is "close" to x_j. By composing analysis operators, we can travel from any level i to any higher level j. This gives an operator

$$\psi_{i,j}^{\uparrow} = \psi_{j-1}^{\uparrow}\psi_{j-2}^{\uparrow}\cdots\psi_i^{\uparrow}, \qquad j > i$$

which maps an element in V_i to an element in V_j. On the other hand, by composing synthesis operators, we can travel from any level j to any lower level i. This gives an operator

$$\psi_{j,i}^{\downarrow} = \psi_i^{\downarrow}\psi_{i+1}^{\downarrow}\cdots\psi_{j-1}^{\downarrow}, \qquad j > i$$

which takes us from level j back to level i. Since the analysis operators are designed to reduce the information content of a signal, they are not invertible in general. In particular, $\psi_j^{\downarrow}\psi_j^{\uparrow}$ will not be the identity operator in general. On the other hand, we always avoid synthesis operators $\psi_j^{\downarrow}$ that reduce information content. In other words, $\psi_j^{\downarrow}$ is taken to be injective. In fact, both conditions are automatically satisfied if we make the following assumption (id denotes the *identity* operator).

Pyramid Condition: The analysis and synthesis operators $\psi_j^{\uparrow}, \psi_j^{\downarrow}$ are said to satisfy the *pyramid condition* if $\psi_j^{\uparrow}\psi_j^{\downarrow} = \mathrm{id}$ on V_{j+1}.

It is easily seen that the pyramid condition implies that $\psi_j^{\uparrow}\psi_j^{\downarrow}\psi_j^{\uparrow} = \psi_j^{\uparrow}$, $\psi_j^{\downarrow}\psi_j^{\uparrow}\psi_j^{\downarrow} = \psi_j^{\downarrow}$, and that $\psi_j^{\downarrow}\psi_j^{\uparrow}$ is idempotent. Now, suppose that all previous conditions are satisfied, and that we have addition and subtraction operators $\dot{+}$, $\dot{-}$ on V_j such that $x_1\dot{+}(x_2\dot{-}x_1) = x_2$, for $x_1, x_2 \in V_j$. Given an input signal $x_0 \in V_0$, we consider the following recursive signal analysis scheme, called the *pyramid transform*:

$$x_0 \to \{x_1, y_0\} \to \{x_2, y_1, y_0\} \to \cdots \to \{x_{k+1}, y_k, y_{k-1}, \cdots, y_0\} \to \cdots$$

where

$$x_{j+1} = \psi_j^{\uparrow}(x_j) \in V_{j+1}$$

and

$$y_j = x_j\dot{-}\psi_j^{\downarrow}(x_{j+1}), \qquad j \geq 0.$$

The original signal $x_0 \in V_0$ can be *exactly* reconstructed from x_{k+1} and $y_0, y_1, \cdots, y_k$ by means of the backward recursion $x_j = \psi_j^{\downarrow}(x_{j+1})\dot{+}y_j$, $j = k, k-1, \cdots, 0$.

III. General Wavelet Decomposition Schemes

In this section, we present a formal definition of a general wavelet decomposition scheme. This scheme encompasses

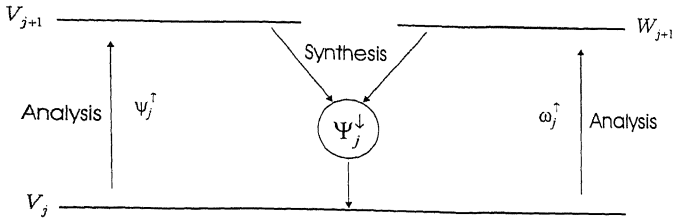

Fig. 1. One stage of the coupled wavelet decomposition scheme.

linear wavelet decompositions as a special case, but allows also a broad class of nonlinear wavelet decomposition schemes. We start in Section III-A with the definition of the so-called coupled wavelet decomposition scheme which comprises two analysis operators, one for the signal and one for the detail, and one synthesis operator. The uncoupled wavelet decomposition scheme introduced in Section III-B is a special case of the coupled wavelet decomposition, in the sense that the synthesis operator is the sum of two synthesis operators, the signal and the detail synthesis operators. The linear wavelet decomposition belongs to this second class; in this case the signal and detail analysis (resp. synthesis) operators correspond to lowpass and highpass analysis (resp. synthesis) operators. In Section V, it will be explained that the lifting scheme provides a practical and flexible method to design both coupled and uncoupled wavelet decomposition schemes.

A. Coupled Wavelet Decomposition

The coupled wavelet decomposition extends the pyramid scheme discussed in Part I; see also Section II. Assume that there exist sets V_j and W_j. We refer to V_j as the *signal space at level* j and to W_j as the *detail space at level* j. Signal analysis consists of decomposing a signal in the direction of increasing j by means of *signal analysis operators* $\psi_j^{\uparrow}: V_j \to V_{j+1}$ and *detail analysis operators* $\omega_j^{\uparrow}: V_j \to W_{j+1}$. On the other hand, *signal synthesis* proceeds in the direction of decreasing j, by means of *synthesis operators* $\Psi_j^{\downarrow}: V_{j+1} \times W_{j+1} \to V_j$. This is illustrated in Fig. 1.

The previous decomposition scheme is required to yield a complete signal representation, in the sense that the mappings $(\psi_j^{\uparrow}, \omega_j^{\uparrow}): V_j \to V_{j+1} \times W_{j+1}$ and $\Psi_j^{\downarrow}: V_{j+1} \times W_{j+1} \to V_j$ are inverses of each other. This leads to the following conditions:

$$\Psi_j^{\downarrow}(\psi_j^{\uparrow}(x), \omega_j^{\uparrow}(x)) = x, \qquad \text{if } x \in V_j \tag{1}$$

which is called the *perfect reconstruction condition*, and

$$\begin{cases} \psi_j^{\uparrow}(\Psi_j^{\downarrow}(x, y)) = x, & \text{if } x \in V_{j+1}, y \in W_{j+1} \\ \omega_j^{\uparrow}(\Psi_j^{\downarrow}(x, y)) = y, & \text{if } x \in V_{j+1}, y \in W_{j+1}. \end{cases} \tag{2}$$

The two conditions in (2) guarantee that the decomposition is nonredundant. Condition (1) implies that the mapping $\Psi_j^{\uparrow}: V_j \to V_{j+1} \times W_{j+1}$, given by $\Psi_j^{\uparrow}(x) = (\psi_j^{\uparrow}(x), \omega_j^{\uparrow}(x))$, is *injective* (i.e., one-to-one) and that $\Psi_j^{\downarrow}$ is *surjective* (i.e., onto). On the other hand, (2) implies that $\Psi_j^{\uparrow}$ is surjective and that $\Psi_j^{\downarrow}$ is injective. Furthermore, if (1) holds and if $\Psi_j^{\uparrow}$ is surjective (or $\Psi_j^{\downarrow}$ is injective) then (2) holds as well. Also, if (2) holds and if $\Psi_j^{\downarrow}$ is surjective (or $\Psi_j^{\uparrow}$ is injective), then (1) holds as well. Now, given an input signal $x_0 \in V_0$, consider the following recursive analysis scheme:

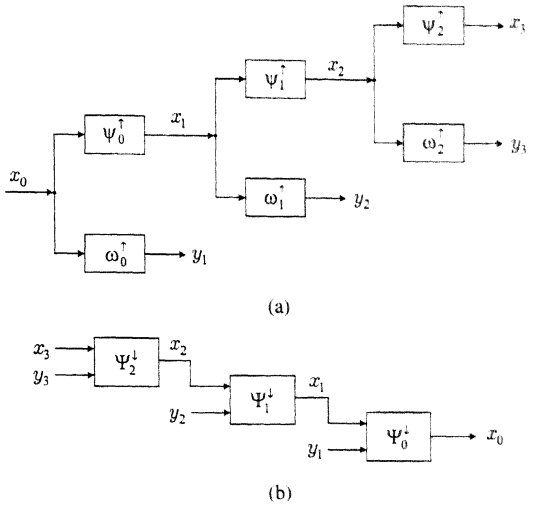

Fig. 2. Three-level coupled wavelet decomposition scheme: (a) signal analysis and (b) signal synthesis.

$$\begin{aligned} x_0 \to \{x_1, y_1\} \to \{x_2, y_2, y_1\} \to \cdots \\ \to \{x_k, y_k, y_{k-1}, \cdots, y_1\} \to \cdots \end{aligned} \tag{3}$$

where

$$x_{j+1} = \psi_j^{\uparrow}(x_j) \in V_{j+1}$$

and

$$y_{j+1} = \omega_j^{\uparrow}(x_j) \in W_{j+1}, \qquad j \geq 0. \tag{4}$$

The original signal x_0 can be *exactly* reconstructed from x_k and $y_1, y_2, \cdots, y_k$ by means of the following recursive synthesis scheme:

$$x_j = \Psi_j^{\downarrow}(x_{j+1}, y_{j+1}), \qquad j = k-1, k-2, \cdots, 0 \tag{5}$$

which shows that the decomposition (3) and (4) is invertible. We refer to the signal representation scheme governed by (1)–(5) as the *coupled wavelet decomposition scheme*. Block diagrams illustrating this scheme, for the case when $k = 3$, are depicted in Fig. 2.

The relationship between the coupled wavelet decomposition scheme and the pyramid scheme discussed in Part I can be easily established. Recall that the latter scheme is governed by the pyramid condition. Let the operators $\psi_j^{\uparrow}, \omega_j^{\uparrow}, \Psi_j^{\downarrow}$ constitute a coupled wavelet decomposition. Fix an element $y_j^0 \in W_j$, for every j, and define $\psi_j^{\downarrow}: V_{j+1} \to V_j$ as $\psi_j^{\downarrow}(x) = \Psi_j^{\downarrow}(x, y_{j+1}^0)$, $x \in V_{j+1}$. Now, the first identity in (2) gives $\psi_j^{\uparrow}(\psi_j^{\downarrow}(x)) = x$, $x \in V_{j+1}$. In other words, the pair $(\psi_j^{\uparrow}, \psi_j^{\downarrow})$ satisfies the pyramid condition.

B. Uncoupled Wavelet Decomposition

Of particular interest is the case when there exists a binary operation $\dot{+}$ on V_j, which we call *addition* (notice that $\dot{+}$ may also depend on j), and operators $\psi_j^{\downarrow}: V_{j+1} \to V_j$ and $\omega_j^{\downarrow}: W_{j+1} \to V_j$ such that

$$\Psi_j^{\downarrow}(x, y) = \psi_j^{\downarrow}(x) \dot{+} \omega_j^{\downarrow}(y), \qquad x \in V_{j+1}, y \in W_{j+1}. \tag{6}$$

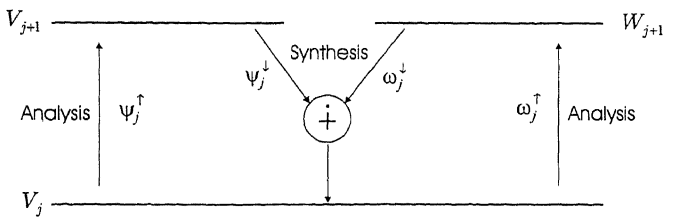

Fig. 3. One stage of the uncoupled wavelet decomposition scheme.

We refer to $\psi_j^{\downarrow}$, $\omega_j^{\downarrow}$ as the *signal synthesis* and the *detail synthesis operators*, respectively. Conditions (1), (2) become

$$\psi_j^{\downarrow}\psi_j^{\uparrow}(x)\dot{+}\omega_j^{\downarrow}\omega_j^{\uparrow}(x) = x, \qquad \text{if } x \in V_j \tag{7}$$

$$\psi_j^{\uparrow}(\psi_j^{\downarrow}(x)\dot{+}\omega_j^{\downarrow}(y)) = x, \qquad \text{if } x \in V_{j+1},\ y \in W_{j+1} \tag{8}$$

$$\omega_j^{\uparrow}(\psi_j^{\downarrow}(x)\dot{+}\omega_j^{\downarrow}(y)) = y, \qquad \text{if } x \in V_{j+1},\ y \in W_{j+1}. \tag{9}$$

We refer to the signal representation scheme governed by (3)–(9) as the *uncoupled wavelet decomposition scheme*. One stage of this scheme is illustrated in Fig. 3.

Given an input signal $x_0 \in V_0$ and the corresponding recursive analysis scheme given in (3) and (4), x_0 can be perfectly reconstructed from x_k and $y_1, y_2, \cdots, y_k$ by means of the following recursive synthesis scheme:

$$x_j = \psi_j^{\downarrow}(x_{j+1})\dot{+}\omega_j^{\downarrow}(y_{j+1}), \qquad j = k-1, k-2, \cdots, 0.$$

Therefore, signal x_j at level j is reconstructed from information that is only available at level $j+1$. First, signal x_{j+1} is mapped down to level j by means of the signal synthesis operator $\psi_j^{\downarrow}$ so as to obtain an approximation $\hat{x}_j = \psi_j^{\downarrow}(x_{j+1})$ of x_j; then, the detail signal y_{j+1} is mapped down to level j by means of the detail synthesis operator $\omega_j^{\downarrow}$ so as to obtain the detail signal $e_j = \omega_j^{\downarrow}(y_{j+1})$ at level j; finally, the results are combined by means of the addition operator $\dot{+}$.

Equation (6) concerns only the structure of the synthesis part. A block diagram illustrating this part, for the case when $k = 3$, is depicted in Fig. 4. The analysis part is the same as in Fig. 2(a).

The linear biorthogonal wavelet transform [30] complies perfectly well with our abstract framework. In [31], we have presented two different ways to view a linear biorthogonal wavelet transform as an uncoupled wavelet decomposition.

In the examples provided below, we consider only one step in the decomposition; i.e., we only consider decompositions between V_0 and V_1, W_1. For simplicity, we delete the subindices $j = 0$ in the corresponding analysis and synthesis operators.

Example 1 (Lazy Wavelet): The simplest example of an uncoupled wavelet decomposition is the transform that splits a 1-D discrete signal $x(n)$ into its odd and even samples. Let $V_0 = V_1 = W_1 = \mathbb{R}^{\mathbb{Z}}$, i.e., the space of doubly infinite real-valued sequences on $\mathbb{Z}$. Then, the analysis operators are given by

$$\psi^{\uparrow}(x)(n) = x(2n) \text{ and } \omega^{\uparrow}(x)(n) = x(2n+1)$$

whereas the synthesis operators are given by

$$\psi^{\downarrow}(x)(2n) = x(n) \text{ and } \psi^{\downarrow}(x)(2n+1) = 0$$
$$\omega^{\downarrow}(y)(2n) = 0 \text{ and } \omega^{\downarrow}(y)(2n+1) = y(n).$$

It is obvious that conditions (7)–(9) are satisfied, with $\dot{+}$ being the standard addition. The lazy wavelet, better known in the signal processing community as the *polyphase transform of order* 2 [32], is not of great interest by itself; the reason why it is discussed here is because it is often used as a starting point for the lifting scheme to be discussed in Section V. ■

Example 2 (S-Transform): The S-transform can be considered as a nonlinear modification of the Haar wavelet with the additional property that it maps integer-valued signals onto integer-valued signals, but without abandoning the property of perfect reconstruction. In this case, the analysis operators are given by

$$\psi^{\uparrow}(x)(n) = \left\lfloor \frac{x(2n) + x(2n+1)}{2} \right\rfloor$$
$$\omega^{\uparrow}(x)(n) = x(2n+1) - x(2n).$$

The corresponding synthesis operators are given by

$$\psi^{\downarrow}(x)(2n) = \psi^{\downarrow}(x)(2n+1) = x(n)$$
$$\omega^{\downarrow}(y)(2n) = -\left\lfloor \frac{y(n)}{2} \right\rfloor \text{ and } \omega^{\downarrow}(y)(2n+1) = \left\lfloor \frac{y(n)+1}{2} \right\rfloor.$$

Here $\lfloor \cdot \rfloor$ denotes the floor function, i.e., for $t \in \mathbb{R}$, $\lfloor t \rfloor$ is the largest integer $\leq t$. Refer to Fig. 5 for an illustration.

The specific character of these operators guarantee that integer signals are mapped onto integer signals, and we may choose $V_0 = V_1 = W_1 = \mathbb{Z}^{\mathbb{Z}}$, i.e., all doubly infinite integer-valued sequences. It is easy to show that conditions (7)–(9) are all satisfied here as well, provided that $\dot{+}$ is taken to be the standard addition.

The S-transform, where "S" stands for "sequential," has been known in the literature for several years, and has been successfully used in medical imaging for lossless compression [33]. During the years, several modifications and generalizations have been proposed, e.g., see [34]. ■

We should point out here that certain continuity issues may arise in the case of an infinite-level wavelet decomposition scheme. However, these issues, which become manifest in the case of infinite decompositions, lie outside the scope of the work presented here, and we choose to limit ourselves to finite-level wavelet decomposition schemes.

C. Nonlinear Biorthogonal-Like Multiresolution Analysis

The linear biorthogonal multiresolution analysis framework [30] can be conceptually extended to the more general framework of the uncoupled wavelet decomposition scheme. Indeed, consider $V_j^{(j+1)} = \text{Ran}(\hat{\psi}_j)$ and $W_j^{(j+1)} = \text{Ran}(\hat{\omega}_j)$, where $\text{Ran}(\psi)$ denotes the *range* of an operator ψ, $\hat{\psi}_j = \psi_j^{\downarrow}\psi_j^{\uparrow}$ and $\hat{\omega}_j = \omega_j^{\downarrow}\omega_j^{\uparrow}$ (recall our discussion and notation in Section II). From (7), we get that every signal $x \in V_j$ has a unique decomposition $x = x'\dot{+}y'$, where $x' \in V_j^{(j+1)}$ and $y' \in W_j^{(j+1)}$, namely $x = \hat{\psi}_j(x)\dot{+}\hat{\omega}_j(x)$. Thus, we may write

$$V_j = V_j^{(j+1)} \bigoplus W_j^{(j+1)}.$$

Let us assume that there exists an $0_v \in V_j$ (which depends on j in general) such that $x\dot{+}0_v = 0_v\dot{+}x = x$, for every $x \in V_j$, and

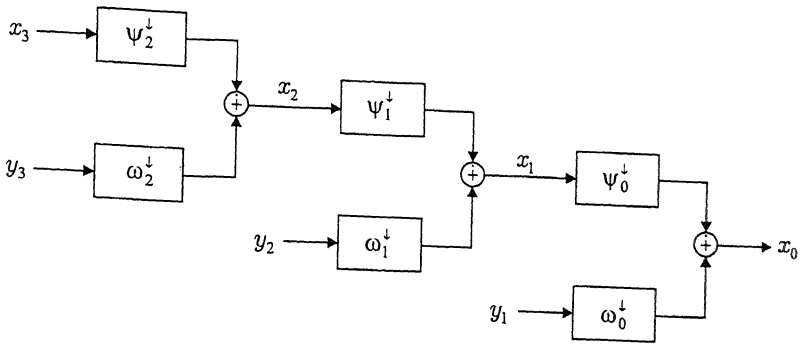

Fig. 4. Signal synthesis part of a three-level uncoupled wavelet decomposition scheme.

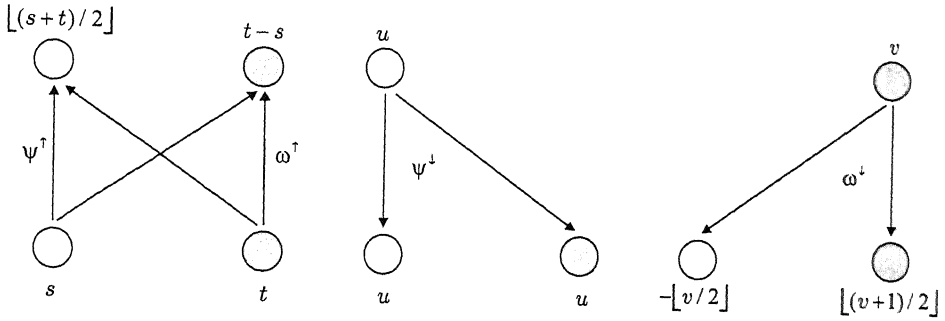

Fig. 5. An illustration of the S-transform. The white and gray nodes correspond to the even and odd samples, respectively.

$\psi_j^{\downarrow}(0_v) = 0_v$. If there exists an $0_w \in W_j$ (which also depends on j in general) such that $\omega_j^{\downarrow}(0_w) = 0_v$, then (8) and (9) imply that

$$\psi_j^{\uparrow}\psi_j^{\downarrow}(x) = x, \quad \text{for } x \in V_{j+1} \tag{10}$$
$$\omega_j^{\uparrow}\omega_j^{\downarrow}(y) = y, \quad \text{for } y \in W_{j+1} \tag{11}$$
$$\psi_j^{\uparrow}\omega_j^{\downarrow}(y) = 0_v, \quad \text{for } y \in W_{j+1} \tag{12}$$
$$\omega_j^{\uparrow}\psi_j^{\downarrow}(x) = 0_w, \quad \text{for } x \in V_{j+1}. \tag{13}$$

This implies that $\hat{\psi}_j$ and $\hat{\omega}_j$ are idempotent operators on V_j (also called *projections*). Furthermore (12) and (13) imply that

$$\hat{\psi}_j\hat{\omega}_j = \hat{\omega}_j\hat{\psi}_j = \underline{0}$$

where $\underline{0}$ is the operator on V_j which is identically 0_v. The projections $\hat{\psi}_j$ and $\hat{\omega}_j$ are *complementary* in the sense that $\hat{\psi}_j \dot{+} \hat{\omega}_j = \mathtt{id}$, where $\mathtt{id}$ denotes the *identity* operator, and $(\hat{\psi}_j \dot{+} \hat{\omega}_j)(x) = \hat{\psi}_j(x) \dot{+} \hat{\omega}_j(x)$, for $x \in V_j$.

IV. Morphological Haar Wavelet

A. One-Dimensional Case

In this section, we discuss a morphological variant of the Haar wavelet in one dimension. The major difference with the classical linear Haar wavelet is that the linear signal analysis filter of the latter is replaced by an erosion (or dilation), i.e., by taking the minimum (or maximum) over two samples. Readers who are unfamiliar with the basic concepts of mathematical morphology are referred to [35], [36].

Let $V_0 = V_1 = W_1 = \mathbb{R}^{\mathbb{Z}}$ be the lattice of doubly infinite real-valued sequences. Define the analysis and synthesis operators as

$$\psi^{\uparrow}(x)(n) = x(2n) \wedge x(2n+1) \tag{14}$$
$$\omega^{\uparrow}(x)(n) = x(2n) - x(2n+1) \tag{15}$$
$$\psi^{\downarrow}(x)(2n) = \psi^{\downarrow}(x)(2n+1) = x(n) \tag{16}$$
$$\omega^{\downarrow}(y)(2n) = y(n) \vee 0,\ \omega^{\downarrow}(y)(2n+1) = -(y(n) \wedge 0). \tag{17}$$

Here "$\wedge$" denotes minimum and "$\vee$" denotes maximum. In Part I, we have seen that the operators $\psi^{\uparrow}$, $\psi^{\downarrow}$ satisfy the pyramid condition. The corresponding pyramid was called the morphological Haar pyramid (see Example 2 in Part I). It can also be shown that (14)–(17) satisfy conditions (7)–(9), provided that $\dot{+}$ is taken to be the standard addition. Therefore, the morphological Haar wavelet is another example of an uncoupled wavelet decomposition scheme.

Fig. 6 illustrates the computations associated with the analysis and synthesis operators of a three-stage morphological Haar wavelet decomposition scheme. The gray nodes indicate the detail signal. Notice that the signal analysis operator guarantees that the range of values of the scaled signals $\{x_j, j \geq 1\}$ is the same as the range of values of the original signal x_0. It furthermore guarantees that, if the original signal x_0 is discrete-valued, the scaled signals $\{x_j, j \geq 1\}$ will be discrete-valued as well, a highly desirable property in lossless coding applications [37]. Moreover, the morphological Haar wavelet decomposition scheme may do a better job in preserving edges in x_0, as compared to the linear case. This is expected, since the signal analysis filters in the linear Haar wavelet decomposition scheme are linear lowpass filters, and as such smooth-out edges. The

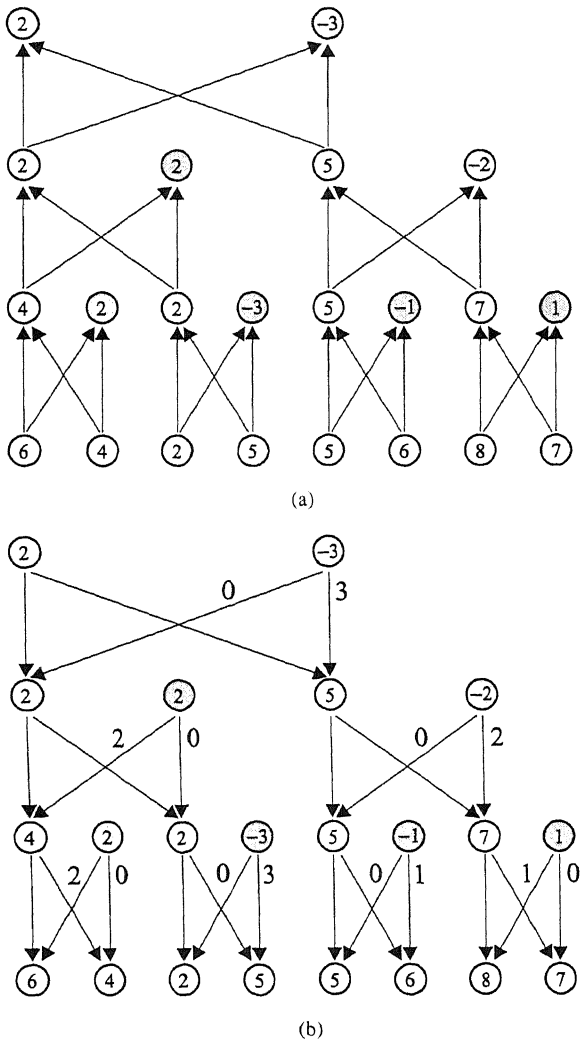

Fig. 6. Computations associated with a three-stage morphological Haar wavelet decomposition scheme: (a) signal analysis and (b) signal synthesis. The gray nodes indicate the detail signal.

signal analysis filters in the morphological Haar case are nonlinear, and as such may preserve edge information.

In (14), we have chosen to use minimum. It is obvious that we can also take maximum instead, i.e., we can set

$$\psi^{\uparrow}(x)(n) = x(2n) \vee x(2n+1)$$

and leave $\omega^{\uparrow}$ unchanged. In this case, the corresponding signal synthesis operator $\psi^{\downarrow}$ is the same as in (16), but the detail synthesis operator becomes

$$\omega^{\downarrow}(y)(2n) = y(n) \wedge 0$$

and

$$\omega^{\downarrow}(y)(2n+1) = -(y(n) \vee 0).$$

Notice that, when we use minimum in the signal analysis operator, $(\psi^{\uparrow}, \psi^{\downarrow})$ is an adjunction, whereas when we use maximum, $(\psi^{\downarrow}, \psi^{\uparrow})$ is an adjunction [36].

It is not difficult to define a binary version of the wavelet decomposition scheme (14)–(17). Indeed, let $V_0 = V_1 = W_1 = \{0, 1\}^{\mathbb{Z}}$ be the Boolean lattice of doubly infinite sequences of 0s and 1s. We choose the "exclusive OR" operation, denoted by $\triangle$, as the binary operation $\dot{+}$ on V_0. Then, we define analysis and synthesis operators [cf. (14)–(17)] as follows:

$$\begin{aligned}
\psi^{\uparrow}(x)(n) &= x(2n) \\
\omega^{\uparrow}(x)(n) &= x(2n) \triangle x(2n+1) \\
\psi^{\downarrow}(x)(2n) &= \psi^{\downarrow}(x)(2n+1) = x(n) \\
\omega^{\downarrow}(y)(2n) &= 0 \text{ and } \omega^{\downarrow}(y)(2n+1) = y(n).
\end{aligned}$$

It is easy to verify that this defines an uncoupled wavelet decomposition scheme. Notice that the detail signal $\omega^{\uparrow}(x)$ contains 1's only at a transition (from 0 to 1 or vice versa) in signal x that occurs at an even point. The decomposition is *self-dual*, in the sense that

$$\psi^{\uparrow}(\overline{x}) = \overline{\psi^{\uparrow}(x)} \text{ and } \omega^{\uparrow}(\overline{x}) = \omega^{\uparrow}(x)$$

where $\overline{x}(n) = 1 - x(n)$. Such a binary scheme can be extended, without serious effort, to finite-valued signals with values in $\{0, 1, \cdots, N-1\}$, $N < \infty$, and with $\triangle$ being replaced by "addition modulo N."

B. Two-Dimensional Case

We can extend the morphological Haar wavelet decomposition scheme to two and higher dimensions by using a separable filter bank (e.g., by sequentially applying the 1-D decomposition on the columns and rows of a 2-D image) [30], [32]. However, we can also define a nonseparable 2-D version of the morphological Haar wavelet. Indeed, let V_0 and V_1 consist of all functions from $\mathbb{Z}^2$ into $\mathbb{R}$ and let W_1 consist of all functions from $\mathbb{Z}^2$ into $\mathbb{R}^3$. We introduce the following notation. By $\boldsymbol{n}$, $2\boldsymbol{n}$ we denote the points (m, n), $(2m, 2n) \in \mathbb{Z}^2$, respectively, and by $2\boldsymbol{n}_+$, $2\boldsymbol{n}^+$, $2\boldsymbol{n}_+^+$ the points $(2m+1, 2n)$, $(2m, 2n+1)$, $(2m+1, 2n+1)$, respectively. Define

$$\psi^{\uparrow}(x)(\boldsymbol{n}) = x(2\boldsymbol{n}) \wedge x(2\boldsymbol{n}_+) \wedge x(2\boldsymbol{n}^+) \wedge x(2\boldsymbol{n}_+^+) \quad (18)$$

$$\omega^{\uparrow}(x)(\boldsymbol{n}) = (\omega_v(x)(\boldsymbol{n}), \omega_h(x)(\boldsymbol{n}), \omega_d(x)(\boldsymbol{n})) \quad (19)$$

where ω_v, ω_h, ω_d represent the vertical, horizontal, and diagonal detail signals, given by

$$\omega_v(x)(\boldsymbol{n}) = \tfrac{1}{2}(x(2\boldsymbol{n}) - x(2\boldsymbol{n}^+) + x(2\boldsymbol{n}_+) - x(2\boldsymbol{n}_+^+)) \quad (20)$$

$$\omega_h(x)(\boldsymbol{n}) = \tfrac{1}{2}(x(2\boldsymbol{n}) - x(2\boldsymbol{n}_+) + x(2\boldsymbol{n}^+) - x(2\boldsymbol{n}_+^+)) \quad (21)$$

$$\omega_d(x)(\boldsymbol{n}) = \tfrac{1}{2}(x(2\boldsymbol{n}) - x(2\boldsymbol{n}_+) - x(2\boldsymbol{n}^+) + x(2\boldsymbol{n}_+^+)). \quad (22)$$

The synthesis operators are now given by

$$\begin{aligned}
\psi^{\downarrow}(x)(2\boldsymbol{n}) &= \psi^{\downarrow}(x)(2\boldsymbol{n}_+) = \psi^{\downarrow}(x)(2\boldsymbol{n}^+) \\
&= \psi^{\downarrow}(x)(2\boldsymbol{n}_+^+) = x(\boldsymbol{n})
\end{aligned} \quad (23)$$

and

$$\begin{aligned}
\omega^{\downarrow}(y)(2\boldsymbol{n}) &= (y_v(\boldsymbol{n}) + y_h(\boldsymbol{n})) \vee (y_v(\boldsymbol{n}) + y_d(\boldsymbol{n})) \\
&\quad \vee (y_h(\boldsymbol{n}) + y_d(\boldsymbol{n})) \vee 0 \\
\omega^{\downarrow}(y)(2\boldsymbol{n}_+) &= (y_v(\boldsymbol{n}) - y_h(\boldsymbol{n})) \vee (y_v(\boldsymbol{n}) - y_d(\boldsymbol{n})) \\
&\quad \vee (-y_h(\boldsymbol{n}) - y_d(\boldsymbol{n})) \vee 0 \\
\omega^{\downarrow}(y)(2\boldsymbol{n}^+) &= (y_h(\boldsymbol{n}) - y_v(\boldsymbol{n})) \vee (-y_v(\boldsymbol{n}) - y_d(\boldsymbol{n})) \\
&\quad \vee (y_h(\boldsymbol{n}) - y_d(\boldsymbol{n})) \vee 0 \\
\omega^{\downarrow}(y)(2\boldsymbol{n}_+^+) &= (-y_v(\boldsymbol{n}) - y_h(\boldsymbol{n})) \vee (y_d(\boldsymbol{n}) - y_v(\boldsymbol{n})) \\
&\quad \vee (y_d(\boldsymbol{n}) - y_h(\boldsymbol{n})) \vee 0
\end{aligned}$$

where we write $y \in W_1$ as $y = (y_v, y_h, y_d)$. It is not difficul to show that conditions (7)–(9) are all satisfied, provided tha

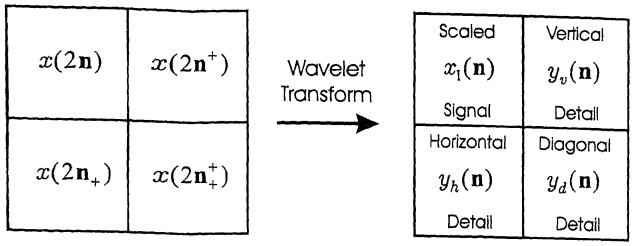

Fig. 7. Two-dimensional Haar wavelet transforms an input signal x to a scaled signal x_1 and the vertical, horizontal, and diagonal detail signals y_v, y_h, y_d, respectively.

$\dot{+}$ is taken to be the standard addition. Therefore, this is a 2-D example of an uncoupled wavelet decomposition scheme.

The analysis operators $\psi^\uparrow$ and $\omega^\uparrow$ in (18) and (19) map a quadruple of signal values, as the ones depicted in the left hand-side of Fig. 7, to the quadruple at the right hand-side; here $x_1 = \psi^\uparrow(x)$ and $y_v = \omega_v(x)$ (the same for y_h, y_d). An example, illustrating one step of this decomposition is depicted in Fig. 8.

As in the 1-D case, the minimum in the expression for $\psi^\uparrow$ can be replaced by a maximum. Moreover, as we explain below, it can also be replaced by any (extension of a) *positive Boolean function* without destroying the condition of perfect reconstruction. Recall that every Boolean function b can be written as a sum-of-products, where the sum represents the "OR" or "maximum" and where the product represents the "AND" or "minimum." If the Boolean function is positive, then this sum-of-products can be written without complemented variables. Such a positive Boolean function can be easily extended from $\{0, 1\}$ to $\mathbb{R}$ by replacing the sum by maximum and the product by minimum [36, Sec. 11.4].

Suppose now that b is a positive Boolean function of four variables and let $\psi^\uparrow$ be given by

$$\psi^\uparrow(x)(\boldsymbol{n}) = b(x(2\boldsymbol{n}), x(2\boldsymbol{n}_+), x(2\boldsymbol{n}^+), x(2\boldsymbol{n}_+^+))$$

and take $\omega^\uparrow$ to be the same as in (19). The value of $b(u_1, u_2, u_3, u_4)$ equals one of its four arguments; which one depends on the ranking of these four elements, and can be deduced from (the signs of) $u_1 - u_2$, $u_1 - u_3$, $u_1 - u_4$. Knowing the value of $b(u_1, u_2, u_3, u_4)$, along with the three differences $u_1 - u_2$, $u_1 - u_3$, $u_1 - u_4$, we are able to compute u_1, u_2, u_3, u_4. This observation can be used to recover the original signal x from $\psi^\uparrow(x)$ and $\omega^\uparrow(x)$. Namely, using (20)–(22), it is easy to show that

$$\begin{aligned} x(2\boldsymbol{n}) - x(2\boldsymbol{n}_+) &= \omega_h(x)(\boldsymbol{n}) + \omega_d(x)(\boldsymbol{n}) \\ x(2\boldsymbol{n}) - x(2\boldsymbol{n}^+) &= \omega_v(x)(\boldsymbol{n}) + \omega_d(x)(\boldsymbol{n}) \\ x(2\boldsymbol{n}) - x(2\boldsymbol{n}_+^+) &= \omega_v(x)(\boldsymbol{n}) + \omega_h(x)(\boldsymbol{n}). \end{aligned}$$

This leads to the signal synthesis operator (23) and to detail synthesis operators that are similar to the ones used by the 2-D version of the morphological Haar wavelet decomposition scheme discussed above. The particular form of the detail synthesis operators depends on the choice for the Boolean function b. Clearly, the resulting wavelet decomposition will be uncoupled.

We can take b to be the kth order statistic of u_1, u_2, u_3, u_4, i.e., the kth value of the sequence of length four obtained by arranging u_1, u_2, u_3, u_4 in decreasing order. Observe that, in this case and for $k = 4$, we obtain the morphological Haar wavelet (and for $k = 1$ its dual). In the following, and for the sake of illustration, we present a 2-D binary example that is built by taking b to be the *median* of the sequence u_1, u_1, u_2, u_3, u_4.

Consider an input signal x, with $x(2\boldsymbol{n}) = a$, $x(2\boldsymbol{n}_+) = b$, $x(2\boldsymbol{n}^+) = c$, and $x(2\boldsymbol{n}_+^+) = d$. The signal analysis operator is given by

$$\begin{aligned} &\psi^\uparrow(x)(\boldsymbol{n}) \\ &\quad = \mathtt{median}(x(2\boldsymbol{n}), x(2\boldsymbol{n}), x(2\boldsymbol{n}_+), x(2\boldsymbol{n}^+), x(2\boldsymbol{n}_+^+)). \end{aligned} \tag{24}$$

Take $\omega^\uparrow$ as in (19), where

$$\omega_v(x)(\boldsymbol{n}) = x(2\boldsymbol{n}) \mathbin{\triangle} x(2\boldsymbol{n}^+) \tag{25}$$

$$\omega_h(x)(\boldsymbol{n}) = x(2\boldsymbol{n}) \mathbin{\triangle} x(2\boldsymbol{n}_+) \tag{26}$$

$$\omega_d(x)(\boldsymbol{n}) = x(2\boldsymbol{n}) \mathbin{\triangle} x(2\boldsymbol{n}_+^+). \tag{27}$$

Referring to Fig. 7, the coefficients in the matrix $\left[\begin{smallmatrix} a & c \\ b & d \end{smallmatrix}\right]$ are mapped to $\left[\begin{smallmatrix} t & v \\ u & w \end{smallmatrix}\right]$, where $t = \mathtt{median}(a, a, b, c, d)$, $u = a \mathbin{\triangle} b$, $v = a \mathbin{\triangle} c$, and $w = a \mathbin{\triangle} d$. It is not difficult to verify that $a = t \mathbin{\triangle} (u \wedge v \wedge w)$, where $t = \mathtt{median}(a, a, b, c, d)$, $u = a \mathbin{\triangle} b$, $v = a \mathbin{\triangle} c$, and $w = a \mathbin{\triangle} d$. To understand this, we distinguish two cases: 1) $u \wedge v \wedge w = 0$: this means that at least one of the values u, v, w equals 0, which implies that at least one of the values b, c, d equals a. This yields that $t = a$, which is in agreement with $a = t \mathbin{\triangle} 0$. 2) $u \wedge v \wedge w = 1$: then $u = v = w = 1$, hence $b = c = d = \bar{a}$. This yields that $t = \bar{a}$. Again, this is in agreement with $a = t \mathbin{\triangle} 1$.

Having a recovered from t, u, v, w, we can recover b from $b = (a \mathbin{\triangle} b) \mathbin{\triangle} a = u \mathbin{\triangle} t \mathbin{\triangle} (u \wedge v \wedge w)$. Similarly, we can find c and d. This leads to synthesis operators, given by (23) and

$$\begin{aligned} \omega^\downarrow(y)(2\boldsymbol{n}) &= y_v(\boldsymbol{n}) \wedge y_h(\boldsymbol{n}) \wedge y_d(\boldsymbol{n}) \\ \omega^\downarrow(y)(2\boldsymbol{n}_+) &= y_h(\boldsymbol{n}) \mathbin{\triangle} (y_v(\boldsymbol{n}) \wedge y_h(\boldsymbol{n}) \wedge y_d(\boldsymbol{n})) \\ \omega^\downarrow(y)(2\boldsymbol{n}^+) &= y_v(\boldsymbol{n}) \mathbin{\triangle} (y_v(\boldsymbol{n}) \wedge y_h(\boldsymbol{n}) \wedge y_d(\boldsymbol{n})) \\ \omega^\downarrow(y)(2\boldsymbol{n}_+^+) &= y_d(\boldsymbol{n}) \mathbin{\triangle} (y_v(\boldsymbol{n}) \wedge y_h(\boldsymbol{n}) \wedge y_d(\boldsymbol{n})). \end{aligned}$$

It is again not difficult to show that conditions (7)–(9) are all satisfied, provided that $\dot{+}$ is taken to be the "exclusive OR" operator. An example, illustrating one step of this decomposition, is depicted in Fig. 9.

V. Lifting Scheme

A useful and very general technique for constructing new wavelet decompositions from existing ones has been recently proposed by Sweldens [23]–[25], and is known as the *lifting scheme*. Lifting amounts to modifying the analysis and synthesis operators in such a way that the properties of the modified scheme are "better" than those of the original one. Here, "better" can be interpreted in different ways. For example, in the linear case, it may mean that the number of vanishing moments is larger. Lifting can be used to construct wavelet decompositions for signals that are defined on arbitrary domains, or to construct nonlinear coupled or uncoupled wavelet decompositions (in the sense of the definitions given in Section III), which is of interest to us. Two types of lifting schemes can be distinguished:

- *Prediction Lifting*. This modifies the detail analysis operator $\omega^\downarrow$ and the signal synthesis operator $\Psi^\downarrow$ in the coupled

Fig. 8. Multiresolution image decomposition based on the 2-D morphological Haar wavelet transform. (a) An image x and (b) its decomposition into the scaled image $\psi^{\uparrow}(x)$, given by (18), and the detail images $\omega_v(x)$, $\omega_h(x)$ and $\omega_d(x)$, given by (20)–(22).

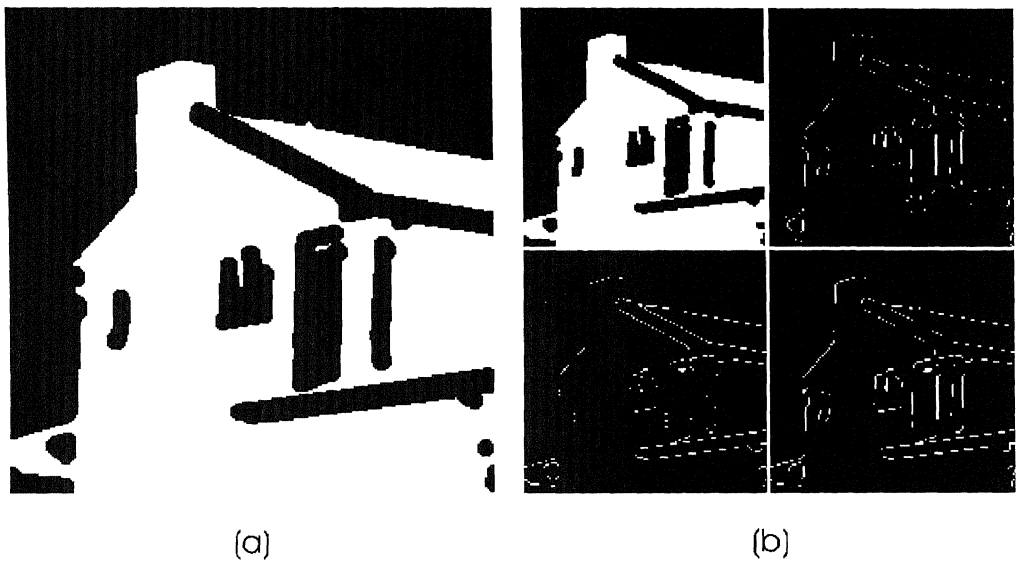

Fig. 9. Multiresolution binary image decomposition based on the 2-D median wavelet transform. (a) Binary image x and (b) its decomposition into the scaled image $\psi^{\uparrow}(x)$, given by (24), and the detail images $\omega_v(x)$, $\omega_h(x)$ and $\omega_d(x)$, given by (25)–(27).

case, or the signal synthesis operator $\psi^{\downarrow}$ in the uncoupled case.

- *Update Lifting.* This modifies the signal analysis operator $\psi^{\uparrow}$ and the signal synthesis operator $\Psi^{\downarrow}$ in the coupled case, or the detail synthesis operator $\omega^{\downarrow}$ in the uncoupled case.

We treat these two cases separately. In both cases, the lifting operator may differ from level to level. However, for simplicity we restrict ourselves to operators between levels 0 and 1.

A. Prediction Lifting

Consider one level of a coupled wavelet decomposition scheme, governed by the analysis operators $\psi^{\uparrow}\colon V_0 \to V_1$, $\omega^{\uparrow}\colon V_0 \to W_1$ and the synthesis operator $\Psi^{\downarrow}\colon V_1 \times W_1 \to V_0$, such that the conditions (1), (2) are satisfied. In many applications, such as data compression, it is desirable to develop wavelet schemes that produce small detail signals $y_1 = \omega^{\uparrow}(x_0)$. Starting from a scheme like above, we might try to decrease the detail signal y_1 by utilizing signal information contained in $x_1 = \psi^{\uparrow}(x_0)$. This may be accomplished by means of a *prediction operator* $\pi\colon V_1 \to W_1$ and a difference operator $\hat{-}$ on W_1 and by setting

$$y_1' = y_1 \hat{-} \pi(x_1) \tag{28}$$

as the new detail signal. This leads to the analysis step depicted in Fig. 10.

Assume now that there exists an addition operator $\hat{+}$ on W_1 such that

$$(y_1 \hat{+} y_2) \hat{-} y_2 = (y_1 \hat{-} y_2) \hat{+} y_2 = y_1, \qquad y_1, y_2 \in W_1. \tag{29}$$

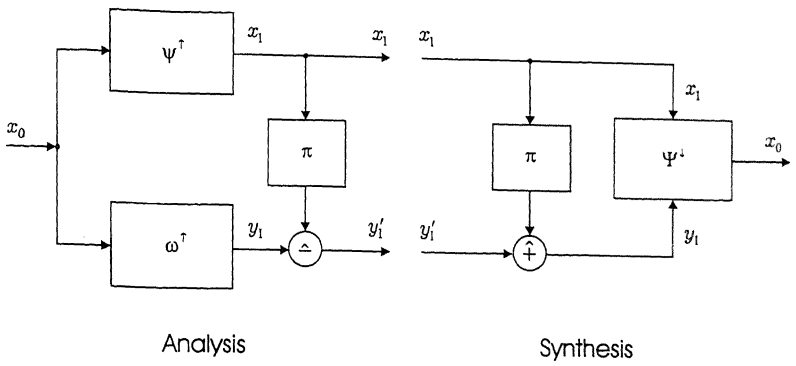

Fig. 10. Analysis and synthesis steps of a prediction lifting scheme.

It is evident that the original signal x_0 can be reconstructed from x_1 and y_1', since

$$x_0 = \Psi^\downarrow(x_1, y_1) = \Psi^\downarrow(x_1, y_1' \hat{+} \pi(x_1)).$$

This leads to the synthesis step depicted in Fig. 10. Thus, we arrive at the *prediction lifting scheme* with analysis and synthesis operators given by

$$\psi_p^\uparrow(x) = \psi^\uparrow(x),\ \omega_p^\uparrow(x) = \omega^\uparrow(x) \hat{-} \pi\psi^\uparrow(x), \qquad x \in V_0 \tag{30}$$

$$\Psi_p^\downarrow(x, y) = \Psi^\downarrow(x, y \dot{+} \pi(x)), \qquad x \in V_1,\ y \in W_1. \tag{31}$$

To show that this defines a coupled wavelet decomposition scheme, we must verify that $\psi_p^\uparrow$, $\omega_p^\uparrow$, and $\Psi_p^\downarrow$ satisfy conditions (1) and (2) as well. Indeed, let $x \in V_0$; then

$$\begin{aligned}&\Psi_p^\downarrow(\psi_p^\uparrow(x), \omega_p^\uparrow(x))\\ &\quad = \Psi^\downarrow(\psi_p^\uparrow(x), \omega_p^\uparrow(x) \hat{+} \pi\psi_p^\uparrow(x))\\ &\quad = \Psi^\downarrow(\psi^\uparrow(x), (\omega^\uparrow(x) \hat{-} \pi\psi^\uparrow(x)) \hat{+} \pi\psi^\uparrow(x))\\ &\quad = \Psi^\downarrow(\psi^\uparrow(x), \omega^\uparrow(x)) = x\end{aligned}$$

where we have used (1) for the original scheme, and (29)–(31). Now, let $x \in V_1$, $y \in W_1$; then

$$\psi_p^\uparrow(\Psi_p^\downarrow(x, y)) = \psi^\uparrow(\Psi^\downarrow(x, y \hat{+} \pi(x))) = x$$

where we have used the first equation in (2) for the original scheme, and (30) and (31). Finally, let $x \in V_1$, $y \in W_1$; then

$$\begin{aligned}&\omega_p^\uparrow(\Psi_p^\downarrow(x, y))\\ &\quad = \omega^\uparrow(\Psi^\downarrow(x, y \hat{+} \pi(x))) \hat{-} \pi\psi^\uparrow(\Psi^\downarrow(x, y \hat{+} \pi(x)))\\ &\quad = (y \hat{+} \pi(x)) \hat{-} \pi(x) = y\end{aligned}$$

where we have used (2) and (29)–(31). In these expressions, $\hat{+}$ and $\hat{-}$ can be the standard addition and subtraction, respectively, but other choices can be envisaged as well. In the binary case, for example, we may choose $\hat{+}$ and $\hat{-}$ to be the exclusive OR. An example will be given in Example 5.

The following result provides some additional properties for the case when the initial wavelet decomposition is uncoupled.

Proposition 1: Consider an uncoupled wavelet decomposition scheme between V_0 and V_1, W_1, with synthesis operators $\psi^\downarrow$, $\omega^\downarrow$, a prediction operator π: $V_1 \to W_1$, and binary operations $\dot{+}$, $\dot{-}$ on W_1 such that (29) is satisfied. Furthermore, assume that

1) binary operator $\dot{+}$ on V_0 is associative and commutative;
2) $\omega^\downarrow$: $W_1 \to V_0$ is "linear," in the sense that

$$\omega^\downarrow(y_1 \hat{+} y_2) = \omega^\downarrow(y_1) \dot{+} \omega^\downarrow(y_2), \qquad y_1, y_2 \in W_1. \tag{32}$$

Then, the prediction-lifted wavelet decomposition, given by (30), (31), is uncoupled (with respect to the same addition operator $\dot{+}$) with synthesis operators

$$\psi_p^\downarrow(x) = \psi^\downarrow(x) \dot{+} \omega^\downarrow\pi(x) \text{ and } \omega_p^\downarrow(y) = \omega^\downarrow(y).$$

Proof: Under the given assumptions, we can write

$$\begin{aligned}\Psi_p^\downarrow(x, y) &= \Psi^\downarrow(x, y \hat{+} \pi(x)) = \psi^\downarrow(x) \dot{+} \omega^\downarrow(y \hat{+} \pi(x))\\ &= \psi^\downarrow(x) \dot{+} (\omega^\downarrow(y) \dot{+} \omega^\downarrow\pi(x))\\ &= (\psi^\downarrow(x) \dot{+} \omega^\downarrow\pi(x)) \dot{+} \omega^\downarrow(y),\end{aligned}$$

which proves the result. ■

Example 3 (Lifting the Morphological Haar Wavelet): Consider the morphological Haar wavelet discussed in Section IV-A. Recall that $V_0 = V_1 = W_1 = \mathbb{R}^{\mathbb{Z}}$ and that $\dot{+}$ is the standard addition. Let $\hat{+}$ and $\hat{-}$ on W_1 be defined by

$$y_1 \hat{+} y_2 = \tfrac{1}{2}(y_1 + y_2) \text{ and } y_1 \hat{-} y_2 = 2y_1 - y_2$$

where $+$, $-$ are the standard addition and subtraction. Obviously, the equalities in (29) are satisfied. Define the prediction operator π: $V_1 \to W_1$ by

$$\pi(x)(n) = x(n) - x(n+1).$$

From (14)–(17), (30) and (31), we obtain a coupled nonlinear wavelet decomposition scheme with analysis and synthesis operators given by

$$\psi_p^\uparrow(x)(n) = x(2n) \wedge x(2n+1) \tag{33}$$

$$\begin{aligned}\omega_p^\uparrow(x)(n) &= 2(x(2n) - x(2n+1)) - (x(2n) \wedge x(2n+1))\\ &\quad + (x(2n+2) \wedge x(2n+3))\end{aligned} \tag{34}$$

$$\Psi_p^\downarrow(x, y)(2n) = x(n) + [\tfrac{1}{2}(y(n) + x(n) - x(n+1)) \vee 0] \tag{35}$$

$$\Psi_p^\downarrow(x, y)(2n+1) = x(n) - [\tfrac{1}{2}(y(n) + x(n) - x(n+1)) \wedge 0]. \tag{36}$$

This scheme has two "vanishing moments" as opposed to the morphological Haar wavelet that has only one. By one "vanishing moment" we mean that a constant input signal $x(n) = b$ produces a zero detail signal, whereas by two "vanishing moments" we mean that a linear signal $x(n) = an + b$ produces a zero detail signal. This is illustrated in Fig. 11. Observe that the wavelet transform in (33), (34) maps integer-valued signals onto integer-valued signals. ■

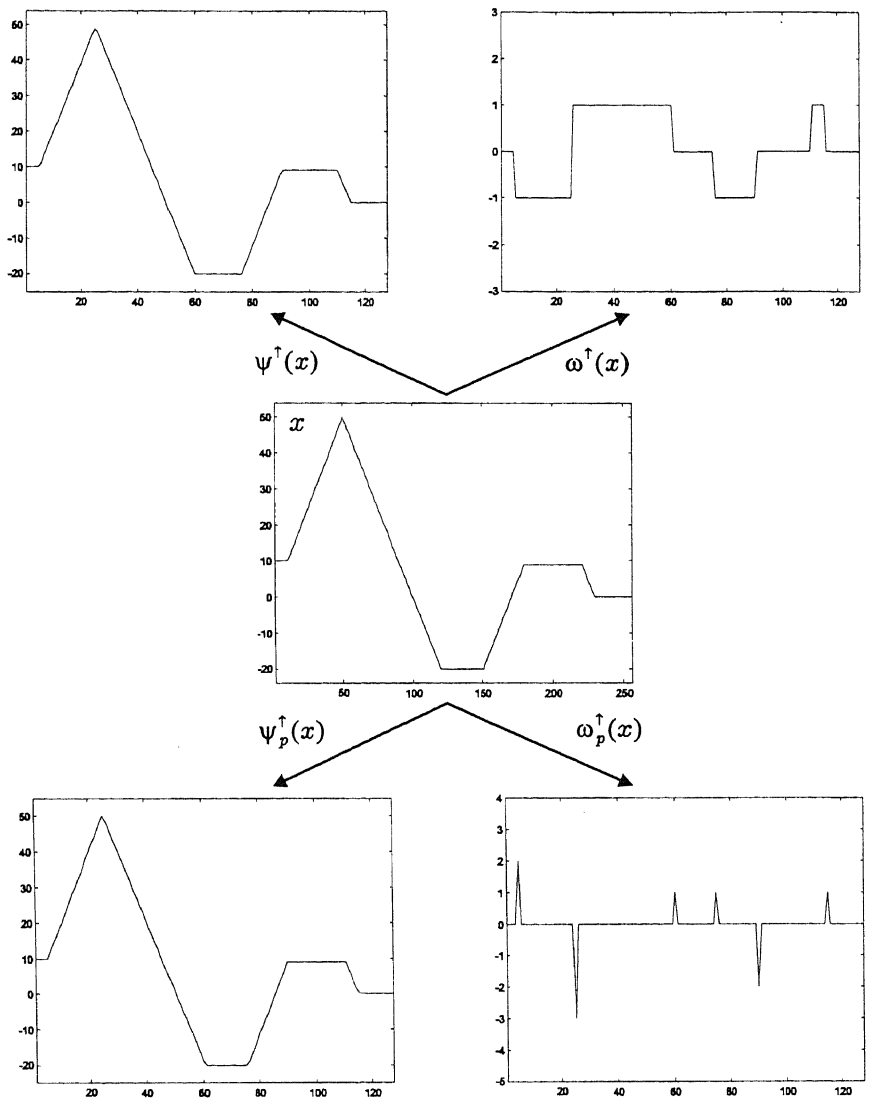

Fig. 11. Morphological Haar wavelet decomposition scheme, with analysis operators $\psi^{\uparrow}$, $\omega^{\uparrow}$, as compared to the wavelet decomposition scheme (33), (34) obtained after prediction lifting. Notice that $\omega^{\uparrow}(x)$ is zero at points where the input signal is constant, whereas $\omega_p^{\uparrow}(x)$ is zero at points where the input signal is linear.

B. Update Lifting

Instead of modifying the detail signal y_1, as we did in (28), we may choose to modify the scaled signal x_1 using the information in y_1. We assume that there exist addition and subtraction operators $\dot{+}$, $\dot{-}$ on V_1 such that

$$(x_1 \dot{+} x_2) \dot{-} x_2 = (x_1 \dot{-} x_2) \dot{+} x_2 = x_1, \; x_1, x_2 \in V_1. \quad (37)$$

We get a modified scaled signal by setting

$$x_1' = x_1 \dot{-} \lambda(y_1). \quad (38)$$

Here, λ is an operator, mapping W_1 into V_1, called the *update operator*. Although, in principle, every mapping λ can be allowed as an update operator, in practice we choose λ in such a way that the resulting scaled signal satisfies a certain constraint. In the linear case, it is often required that the resulting analysis filter $x_0 \mapsto x_1'$ is a lowpass filter. Alternatively, we may require that this mapping preserves a given signal attribute (e.g., average or maximum). If the unmodified scaled signal x_1 does not satisfy the constraint, we may choose λ in such a way that x_1', given by (38), does satisfy this constraint. We refer to the work of Sweldens [23]–[25] and Daubechies and Sweldens [38] for more details.

The update step in (38) gives rise to the diagrams depicted in Fig. 12. It is clear that the input signal x_0 can be reconstructed from x_1' and y_1, since

$$x_0 = \Psi^{\downarrow}(x_1, y_1) = \Psi^{\downarrow}(x_1' \dot{+} \lambda(y_1), y_1).$$

Thus, we arrive at the *update lifting scheme* with analysis and synthesis operators given by

$$\psi_u^{\uparrow}(x) = \psi^{\uparrow}(x) \dot{-} \lambda\omega^{\uparrow}(x), \; \omega_u^{\uparrow}(x) = \omega^{\uparrow}(x), \qquad x \in V_0 \quad (39)$$

$$\Psi_u^{\downarrow}(x, y) = \Psi^{\downarrow}(x \dot{+} \lambda(y), y), \qquad x \in V_1, \; y \in W_1. \quad (40)$$

In the same way as we did for the prediction lifting scheme, we can show that (39) and (40) defines a coupled wavelet decompo-

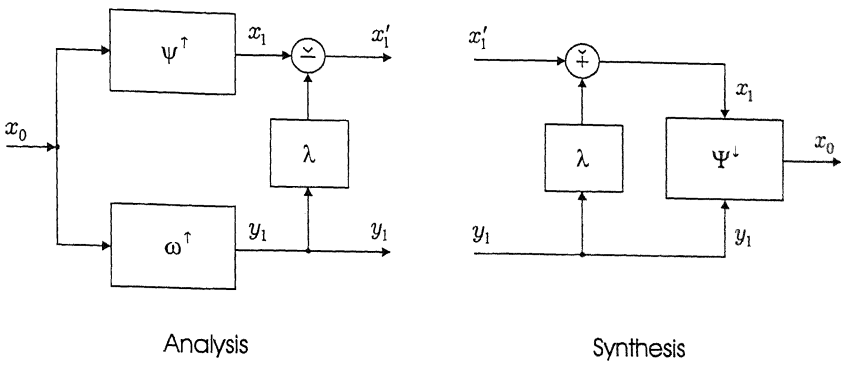

Fig. 12. Analysis and synthesis steps of an update lifting scheme.

sition scheme. Furthermore, the following analogue to Proposition 1 can be established.

Proposition 2: Consider an uncoupled wavelet decomposition scheme between V_0 and V_1, W_1, with synthesis operators $\psi^{\downarrow}$, $\omega^{\downarrow}$, an update operator λ: $W_1 \to V_1$, and binary operations $\dot{+}$, $\check{-}$ on V_1 such that (37) is satisfied. Furthermore, assume that

1) binary operator $\dot{+}$ on V_0 is associative and commutative;
2) $\psi^{\downarrow}$: $V_1 \to V_0$ is "linear," in the sense that

$$\psi^{\downarrow}(v_1 \check{+} v_2) = \psi^{\downarrow}(v_1) \dot{+} \psi^{\downarrow}(v_2), \qquad v_1, v_2 \in V_1. \tag{41}$$

Then, the update-lifted wavelet decomposition, given by (39) and (40), is uncoupled (with respect to the same addition operator $\dot{+}$) with synthesis operators

$$\psi_u^{\downarrow}(x) = \psi^{\downarrow}(x) \text{ and } \omega_u^{\downarrow}(y) = \omega^{\downarrow}(y) \dot{+} \psi^{\downarrow}\lambda(y).$$

In the following example we build a nonlinear wavelet scheme by concatenation of a prediction and an update lifting step.

Example 4 (Lifting Based on the Median Operator): Let us take $\hat{-}$, $\check{-}$ to be the standard subtraction, and $\hat{+}$, $\check{+}$, $\dot{+}$ to be the standard addition. Consider the case of a prediction-update lifting scheme with initial signal decomposition given by means of the lazy wavelet, and prediction and update operators given by

$$\pi(x)(n) = x(n),\ \lambda(y)(n) = -\texttt{median}(0,\ y(n-1),\ y(n)). \tag{42}$$

We obtain an uncoupled wavelet decomposition scheme, with analysis and synthesis operators given by

$$\begin{aligned}&\psi_{pu}^{\uparrow}(x)(n)\\ &\quad = x(2n) + \texttt{median}\\ &\qquad \cdot (0,\ x(2n-1) - x(2n-2),\ x(2n+1) - x(2n))\end{aligned} \tag{43}$$

$$\begin{aligned}&\omega_{pu}^{\uparrow}(x)(n)\\ &\quad = x(2n+1) - x(2n)\end{aligned} \tag{44}$$

$$\begin{aligned}&\psi_{pu}^{\downarrow}(x)(2n)\\ &\quad = \psi_{pu}^{\downarrow}(x)(2n+1) = x(n)\end{aligned} \tag{45}$$

$$\begin{aligned}&\omega_{pu}^{\downarrow}(y)(2n)\\ &\quad = -\texttt{median}(0,\ y(n-1),\ y(n))\\ &\omega_{pu}^{\downarrow}(y)(2n+1)\\ &\quad = y(n) - \texttt{median}(0,\ y(n-1),\ y(n)).\end{aligned} \tag{46}$$

Notice that, the update operator adjusts the value of $x(2n)$ based on the local structure of the input signal $x(n)$. If the difference $x(2n-1)-x(2n-2)$ is negative (or positive) and the difference $x(2n+1)-x(2n)$ is positive (or negative), then no adjustment is made. This happens, for example, when $x(2n)$ is a local minimum (or maximum), as illustrated in Fig. 13(a). If however both differences $x(2n-1)-x(2n-2)$ and $x(2n+1)-x(2n)$ are negative (or positive), then $x(2n)$ is adjusted by adding the smallest (in absolute value) difference. For example, when $x(n)$ (locally) oscillates between two values, as depicted in Fig. 13(b), then (43) will bring $x(2n)$ in line with $x(2n-1)$, thus getting a scaled signal $\psi_{pu}^{\uparrow}(x)$ that approximates x "better" than the scaled signal $\psi^{\uparrow}(x)$ before prediction-update lifting. Concerning the last property, one may observe that it holds for positive as well as for negative constants c.

Alternatively, we may choose

$$\pi(x)(n) = \tfrac{1}{2}(x(n) + x(n+1))$$

and $\lambda(y)$ as in (42). This choice leads to an uncoupled wavelet decomposition scheme that has two "vanishing moments," in the sense that the detail signal, resulting from an input signal $x(n) = an + b$, will be zero.

Finally, one can replace the previous linear prediction operator, with the nonlinear prediction operator

$$\pi(x)(n) = \texttt{median}(x(n-1),\ x(n),\ x(n+1)).$$

This choice, together with (42) for the update operator, leads to a coupled wavelet decomposition scheme. ■

Example 5 (Lifting Binary Wavelets): Let us now consider the binary case, for which $V_0 = V_1 = W_1 = \{0, 1\}^{\mathbb{Z}}$. The previous example, based on the median operator, can be reformulated for binary signals as well. For this case, we take $\hat{-}$, $\check{-}$, $\hat{+}$, $\check{+}$, $\dot{+}$ to be the "exclusive OR" operator $\triangle$. We can now proceed with a prediction-update lifting scheme, with initial signal decomposition given by means of the lazy wavelet and prediction and update operators given by

$$\begin{aligned}&\pi(x)(n) = x(n)\\ &\lambda(y)(n) = \texttt{median}(0,\ y(n-1),\ y(n)) = y(n) \wedge y(n-1).\end{aligned}$$

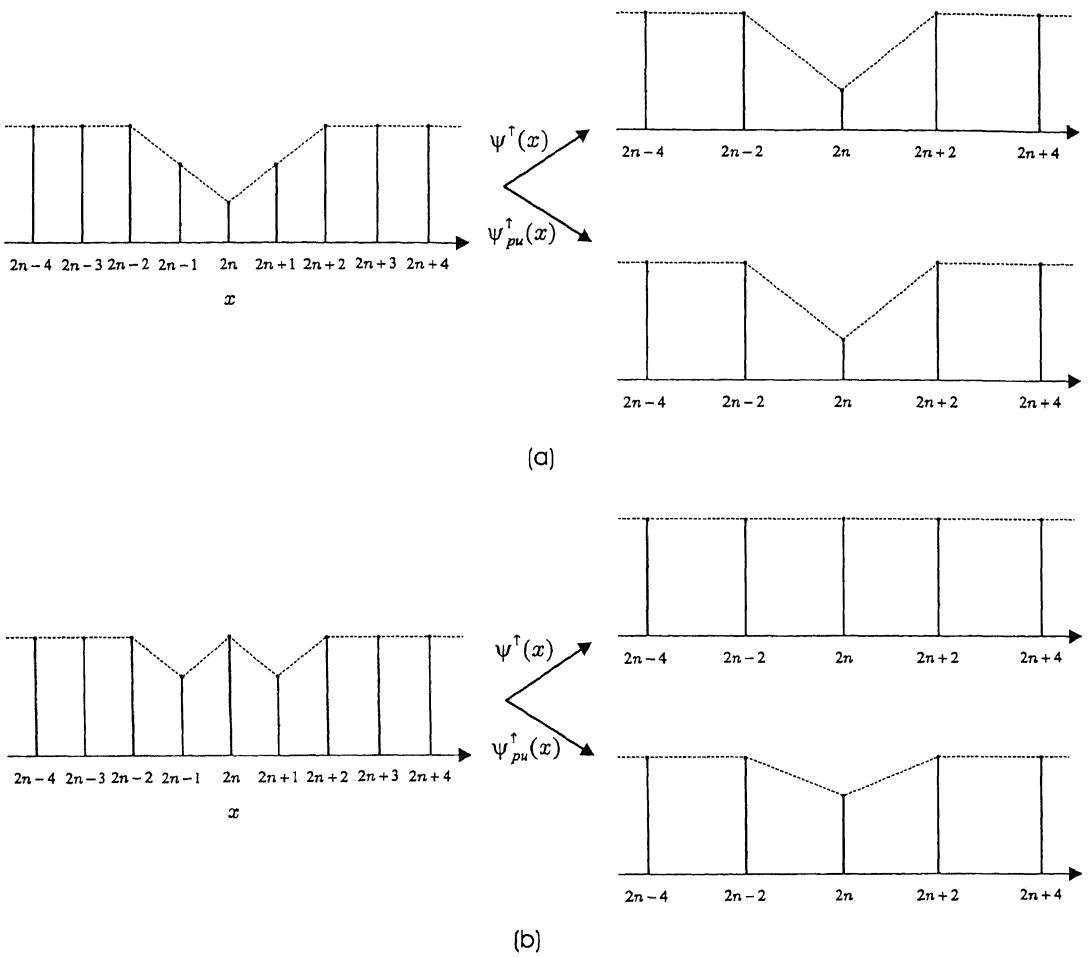

Fig. 13. Illustration of update lifting by means of (43). (a) Since $x(2n)$ is a local minimum in x, (43) maps $x(2n)$ into itself. (b) Since $x(2n-1)-x(2n-2)=x(2n+1)-x(2n)=-1$, the value $x(2n)$ is reduced by one, thus obtaining a scaled signal $\psi^{\uparrow}_{pu}(x)$ that approximates x "better than the scaled signal $\psi^{\uparrow}(x)$ before prediction-update lifting.

Notice that $\texttt{median}(0,\, s,\, t) = s \wedge t$, for $s,\, t \in \{0,\, 1\}$. The analysis and synthesis operators resulting from this lifting scheme can be expressed as

$$\begin{aligned}
&\psi^{\uparrow}_{pu}(x)(n)\\
&\quad = a^{\uparrow}(x(2n-2),\, x(2n-1),\, x(2n),\, x(2n+1))\\
&\omega^{\uparrow}_{pu}(x)(n)\\
&\quad = b^{\uparrow}(x(2n-2),\, x(2n-1),\, x(2n),\, x(2n+1))\\
&\Psi^{\downarrow}_{pu}(x,\, y)(2n)\\
&\quad = a^{\downarrow}(x(n),\, y(n-1),\, y(n))\\
&\Psi^{\downarrow}_{pu}(x,\, y)(2n+1)\\
&\quad = b^{\downarrow}(x(n),\, y(n-1),\, y(n))
\end{aligned}$$

where $a^{\uparrow}$, $b^{\uparrow}$, $a^{\downarrow}$, $b^{\downarrow}$ are Boolean functions given by

$$\begin{aligned}
a^{\uparrow}(u_1,\, u_2,\, u_3,\, u_4) &= u_3 + (u_1 + u_2 - 2u_1u_2)(u_4 - u_3)\\
b^{\uparrow}(u_1,\, u_2,\, u_3,\, u_4) &= u_3 + u_4 - 2u_3u_4\\
a^{\downarrow}(u_1,\, u_2,\, u_3) &= u_1 + (1-2u_1)u_2u_3\\
b^{\downarrow}(u_1,\, u_2,\, u_3) &= u_1 + (1-2u_1)(1-u_2)u_3.
\end{aligned}$$

Clearly, the resulting wavelet decomposition scheme is coupled and *self-dual*, in the sense that

$$\psi^{\uparrow}_{pu}(\overline{x}) = \overline{\psi^{\uparrow}_{pu}(x)} \text{ and } \omega^{\uparrow}_{pu}(\overline{x}) = \omega^{\uparrow}_{pu}(x)$$

where $\overline{x}(n) = 1 - x(n)$. ■

We now mention the following important consequence of Proposition 1 and Proposition 2. If the wavelet decomposition used as a starting point for lifting is uncoupled and "linear," in the sense that the synthesis operators $\omega^{\downarrow}$, $\psi^{\downarrow}$ satisfy (32), (41), if the binary operators $\hat{+}$, $\check{+}$ (on W_1 and V_1) satisfy (29), (37), and if the binary operator $+$ on V_0 is associative and commutative, then the resulting scheme after one lifting step (prediction or update) is also uncoupled. However, after a second lifting step (of the opposite type) the scheme will become coupled in general. This implies that prediction-update and update-prediction lifting schemes will in general give rise to coupled wavelet decompositions, even if all assumptions associated with Proposition 1 and Proposition 2 are satisfied. For example, prediction lifting as described in Proposition 1 yields a modified synthesis operator $\psi^{\downarrow}_{p}$ which is no longer "linear" and thus Proposition 2 is not applicable to the prediction lifted scheme.

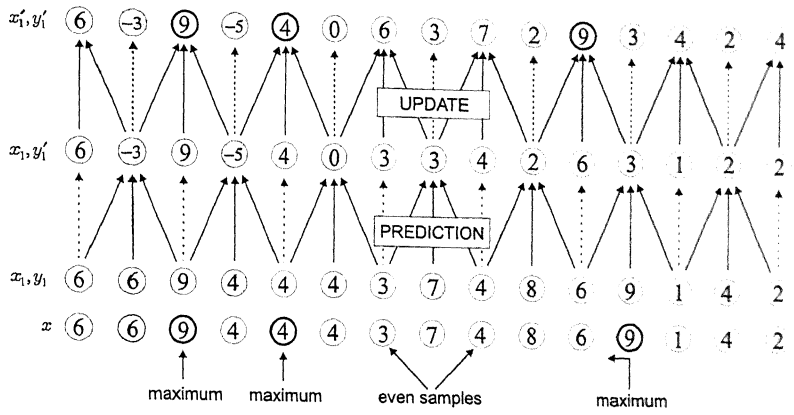

Fig. 14. Diagram illustrating the 1-D max-lifting scheme. The white nodes contain the scaled signal x_1 (resp. x_1'), whereas the gray nodes contain the detail signal y_1 (resp. y_1'). The first lifting step (prediction) modifies the detail signal, whereas the second lifting step (update) modifies the scaled signal such that local maxima are preserved. The initial decomposition $x \mapsto x_1, y_1$ is done by means of the lazy wavelet.

Finally, we point out that Daubechies and Sweldens [38] have shown that linear wavelet transforms can be decomposed into lifting steps. To what extent such a result can be generalized to the nonlinear case remains to be seen.

VI. Max- and Min-Lifting Schemes

In this section, we briefly discuss a particular example of a wavelet decomposition, by means of prediction-update lifting, that leads to the so-called *max-lifting* scheme. More details on this scheme will be provided in a forthcoming paper. We take $\hat{-}$, $\check{-}$ to be standard subtraction, $\hat{+}$, $\check{+}$, $+$ to be standard addition, and we choose prediction and update operators as

$$\pi(x)(n) = x(n) \vee x(n+1), \; \lambda(y)(n) = -(0 \vee y(n-1) \vee y(n)).$$

In this case

$$y_1'(n) = y_1(n) - (x_1(n) \vee x_1(n+1)) \text{ (prediction)} \quad (47)$$
$$x_1'(n) = x_1(n) + (0 \vee y_1'(n-1) \vee y_1'(n)) \text{ (update)}. \quad (48)$$

Thus, as a prediction for $y_1(n)$ we choose the maximum of its two neighbors in x_1, i.e., $x_1(n)$ and $x_1(n+1)$. The update step is chosen in such a way that local maxima of the input signal x_1 are mapped to the scaled signal x_1' (see below). Here, a signal x is said to have a local maximum at n if $x(n) \geq x(n \pm 1)$. The max-lifting scheme yields a coupled wavelet decomposition. This is in agreement with observations made before, since the max-lifting scheme is constructed by means of two nonlinear lifting steps.

Given an input signal x, let x_1, y_1 be the corresponding lazy wavelet decomposition [i.e., $x_1(n) = x(2n)$ and $y_1(n) = x(2n+1)$], and let x_1', y_1' be the output given by the max-lifting wavelet decomposition. The following properties can be established [31]:

1) If x has a local maximum at $2n$, then x_1' has a local maximum at n with $x_1'(n) = x(2n)$.
2) Suppose that $x(2n+1) \geq x(2n+1+i)$, for $-2 \leq i \leq 2$. Then, x_1' has a local maximum at n or $n+1$ with value $x(2n+1)$ depending on which value is the largest, $x(2n)$ or $x(2n+2)$.
3) If x_1' has a local maximum at n, then x has a local maximum at $m \in \{2n-1, 2n, 2n+1\}$ and $x_1'(n) = x(m)$.

Refer to Fig. 14 for an illustration. Properties 1) and 2) mean that local maxima of the input signal x are mapped to the scaled signal x_1'. Property 3), on the other hand, guarantees that no new local maxima of the signal are being created by the scheme.

If we replace the maximum in (47) and (48) with minimum, we obtain the dual scheme, which we refer to as the *min-lifting scheme*. The previous properties can be modified accordingly, by replacing $\geq$ with $\leq$ and "maximum" with "minimum."

We can extend the max- and min-lifting schemes to two dimensions by sequentially applying the 1-D decomposition on the columns and rows of a 2-D image. Fig. 15 depicts the result of a single level wavelet image decomposition by means of max-lifting. Notice that the decomposition produces one scaled image and three detail images (a horizontal, vertical, and diagonal detail image). Notice also that the detail signals are zero (or almost zero) at areas of smooth graylevel variation, and that sharp graylevel variations are mapped to negative (black) detail signal values.

Example 6: We now illustrate the 1-D max-lifting and min-lifting schemes, applied on a signal $x_0(n)$ of 512 samples, and demonstrate the potential of these schemes for extracting regions of stationary signal behavior. We may assume that a signal $x_0(n)$ consists of noise, representing signal variation within a region, superimposed on a piecewise constant signal $s_0(n)$, representing regions of stationary signal behavior. We are interested in obtaining an approximation $\hat{s}_0$ of s_0 from given data x_0.

A very important observation here is that the max-lifting scheme preserves the number and shapes of flat regions in a piecewise constant signal. This is a direct consequence of the fact that this scheme preserves local maxima and, moreover, it does not create new ones. It is therefore expected that max-lifting will preserve, over a range of scales, the number and shapes of regions of constant signal value. Fig. 16 depicts the results of seven experiments based on a three-level linear wavelet decomposition scheme, a four-level max-lifting scheme, and a four-level min-lifting scheme. Our computations consist of three steps: 1) signal analysis $x_0 \mapsto \{x_k, y_k, y_{k-1}, \cdots, y_1\}$, 2) filtering of the detail signals $y_j \mapsto \overline{y}_j$, for $j = 1, 2, \cdots, k$, and 3) signal synthesis

Fig. 15. Single-level separable image decomposition by means of max-lifting.

$\{x_k, \overline{y}_k, \overline{y}_{k-1}, \cdots, \overline{y}_1\} \mapsto \overline{x}_0 = \hat{s}_0$. Fig. 16(a) depicts a signal x_0 with regions of stationary signal behavior, depicted by the signal $s_0(n)$ plotted with a thick line. In this case, the noise component has been generated by smoothing (with a four-tap averaging mask $[1/4, 1/4, 1/4, 1/4]$) zero mean white Gaussian noise with unit variance. Fig. 16(b) depicts the signal $\hat{s}_0$ (plotted with a thick line), obtained by means of a three-level linear denoising scheme [the use of a denoising scheme is justified here by considering $s_0(n)$ as the noise-free signal to be recovered by means of denoising, and the signal variation within a particular signal region as noise to be removed by denoising]. This scheme performs a three-level signal analysis by using the *Symmlet-8* wavelet [30], filters the detail signals by means of the *soft thresholding* operator $\overline{y}(n) = \text{sign}(y(n))(|y(n)| - t)$, if $|y(n)| > t$, and $\overline{y}(n) = 0$, if $|y(n)| \leq t$, where $t = \gamma\sqrt{2 * \ln N}$ [39], and produces signal $\hat{s}_0$ by means of signal synthesis based on the filtered detail signals. We set $\gamma = 1$. It is worthwhile noticing that, although signal variation has been substantially reduced, the reconstructed signal $\hat{s}_0$ fails to capture the staircase structure of signal s_0. This is mainly due to the linear nature of the wavelet decomposition scheme used. The signal $\hat{s}_0$ depicted in Fig. 16(c) has been obtained by using the max-lifting scheme with $\overline{y}(n) = y(n) \vee 0$, whereas, Fig. 16(d) depicts the signal $\hat{s}_0$ obtained by using the min-lifting scheme with $\overline{y}(n) = y(n) \wedge 0$. By taking $\overline{y}(n) = y(n) \vee 0$, we preserve positive detail signal information, whereas we discard negative information (i.e., we apply *max-thresholding*). By taking $\overline{y}(n) = y(n) \wedge 0$, we preserve negative detail signal information, whereas we discard positive information (i.e., we apply *min-thresholding*). Notice that the signal $\hat{s}_0$ depicted in Fig. 16(c) is larger than the original signal $x_0(n)$ [i.e., $\hat{s}_0$ is like an "upper envelope" for $x_0(n)$]. In [31], we have shown that the corresponding operator $x_0 \mapsto \hat{s}_0$ is a morphological closing, and it is therefore extensive. The signal $\hat{s}_0$ depicted in Fig. 16(d) is smaller than signal $x_0(n)$ [i.e., $\hat{s}_0$ is like a "lower envelope" for $x_0(n)$]. On the other hand, Fig. 16(e) depicts the signal $\hat{s}_0$ obtained by using the max-lifting scheme with soft thresholding (with $\gamma = 1$), whereas the signal $\hat{s}_0$ depicted in Fig. 16(f) has been obtained by means of the min-lifting scheme with soft thresholding (with $\gamma = 1$). Fig. 16(g) depicts the signal $\hat{s}_0$ obtained by means of applying max-lifting on x_0 with max-thresholding, followed by min-lifting with min-thresholding. On the other hand, Fig. 16(h) depicts the signal $\hat{s}_0$ obtained by means of applying max-lifting on x_0, followed by min-lifting; denoising is obtained by applying soft thresholding on the detail signals (with $\gamma = 0.4$), in the same manner as in Fig. 16(e) and (f). Notice that, in both cases, signal variation has been substantially reduced, whereas the resulting signal successfully captures the staircase nature of signal s_0. ■

VII. Conclusions and Final Remarks

The main objective of the work presented in this paper was to provide a rigorous theoretical approach to the problem of nonlinear wavelet decomposition and develop tools that can be effectively used for building nonlinear multiresolution signal decomposition schemes that are nonredundant and guarantee perfect reconstruction. The nonlinear schemes discussed as examples in this paper enjoy some useful and attractive properties.

1) Implementation can be done extremely fast by means of simple operations (e.g., addition, subtraction, max, min, median, etc.). This is partially due to the fact that only integer arithmetic is used in calculations and that use of prediction/update steps in the decomposition produces computationally efficient implementations.
2) If the input to the proposed schemes is integer-valued, the output will be integer-valued as well. Clearly, these schemes can avoid quantization, an attractive property for lossless data compression.
3) The proposed schemes can be easily adapted to the case of binary images. This is of particular interest to document image processing, analysis, and compression applications (and other industrial applications) and is important on its own right (e.g., see [40] for a recent work on constructing wavelet decomposition schemes for binary images).
4) Due to the nonlinear nature of the proposed signal analysis operators, important geometric information (e.g., edges) is well preserved at lower resolutions. In the case of the max- (min-) lifting schemes, for example,

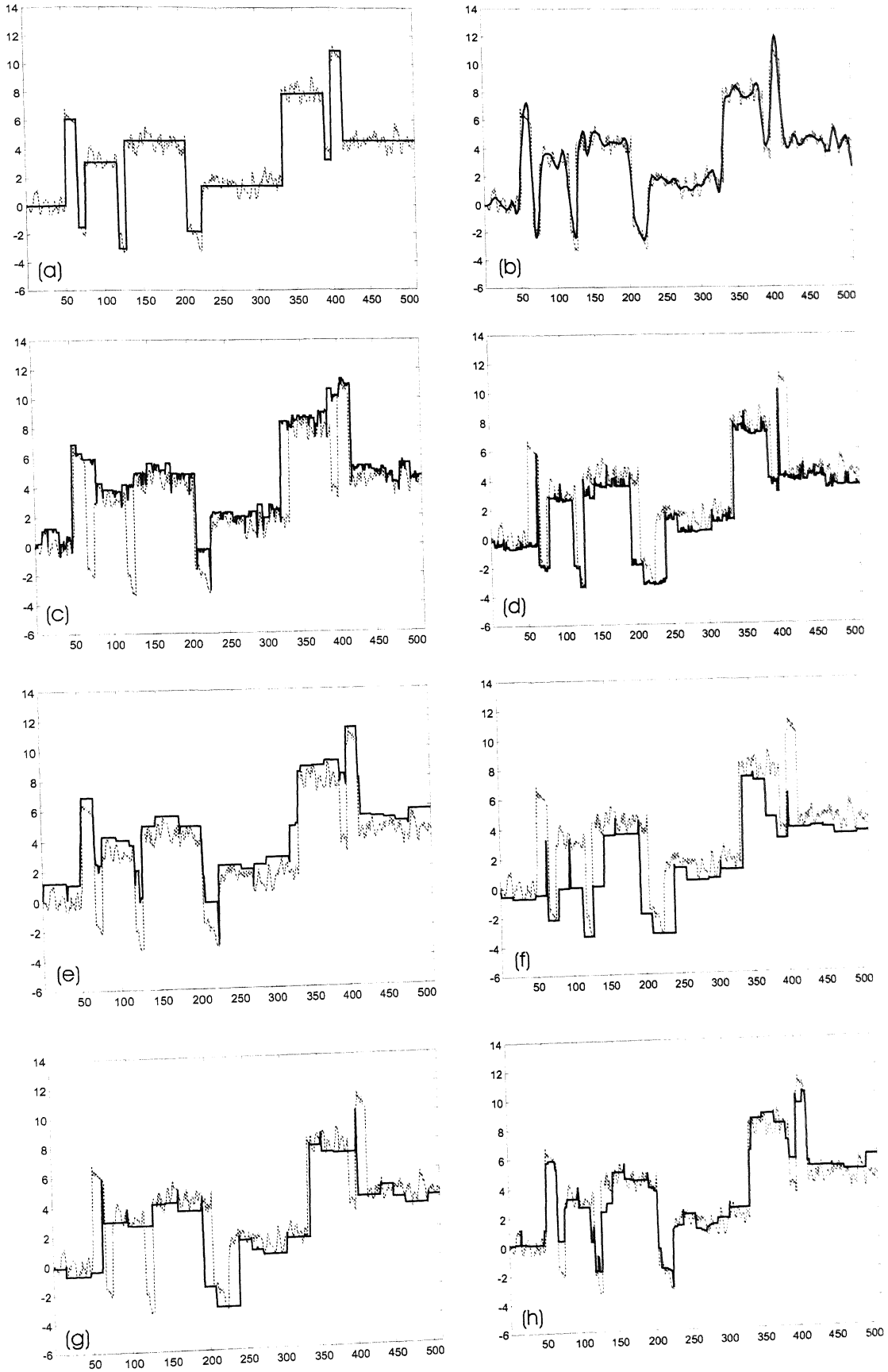

Fig. 16. (a) Signal x_0 with regions of stationary signal behavior (plotted with a thick line). The result of applying on x_0 a denoising scheme based on: (b) the Symmlet-8 wavelet with soft thresholding, (c) max-lifting with max-thresholding, (d) min-lifting with min-thresholding, (e) max-lifting with soft thresholding, (f) min-lifting with soft thresholding, (g) max-lifting with max-thresholding followed by min-lifting with min-thresholding, and (h) max-lifting with soft thresholding followed by min-lifting with soft thresholding.

local maxima (minima) are well preserved at lower resolutions. This property may turn out to be particularly useful in wavelet-based pattern recognition approaches as, for example, wavelet-based face recognition schemes [41].

Despite all these attractive properties, a number of open theoretical and practical questions need to be addressed before such tools become useful in signal processing and analysis applications. For example, we need to better understand how to design prediction and update operators that lead to nonlinear wavelet decompositions that satisfy properties key to a given application at hand, e.g., see the max-lifting scheme discussed in Section VI. Another problem of interest is to investigate the relationship between the discrete nonlinear approach presented in this paper and another nonlinear multiresolution approach to signal analysis known as nonlinear (morphological) scale spaces [42]–[46]. In fact, due to the popularity of nonlinear scale spaces in signal analysis, it may be attractive to investigate the design of nonlinear filter banks by means of discretizing continuous morphological scale spaces. Toward this direction, Pouye *et al.* [20] have recently proposed a nonlinear filter bank that is built by discretizing nonlinear *partial differential equations* (PDEs) used in scale-space theory. This is a very interesting approach for constructing nonlinear filter banks that may be compatible with current multiscale signal analysis techniques based on nonlinear PDEs.

ACKNOWLEDGMENT

The authors would like to thank J.-C. Pesquet for interesting and stimulating discussions and suggestions. Moreover, the authors would like to thank the reviewers and P. Moulin, the Associate Editor handling this paper, for their helpful comments and suggestions.

REFERENCES

[1] J. Goutsias and H. J. A. M. Heijmans, "Nonlinear multiresolution signal decomposition schemes—Part I: Morphological pyramids," *IEEE Trans. Image Processing*, vol. 9, pp. 1862–1876, Nov. 2000.

[2] P. J. Burt and E. H. Adelson, "The Laplacian pyramid as a compact image code," *IEEE Trans. Commun.*, vol. 31, pp. 532–540, 1983.

[3] P. Maragos, "Morphological skeleton representation and coding of binary images," *IEEE Trans. Acoust., Speech, Signal Processing*, vol. 34, pp. 1228–1244, 1986.

[4] O. Egger and W. Li, "Very low bit rate image coding using morphological operators and adaptive decompositions," in *Proc. IEEE Int. Conf. Image Processing*, Austin, TX, 1994, pp. 326–330.

[5] D. A. F. Florêncio and R. W. Schafer, "A nonexpansive pyramidal morphological image coder," in *Proc. IEEE Int. Conf. Image Processing*, Austin, TX, 1994, pp. 331–335.

[6] O. Egger, W. Li, and M. Kunt, "High compression image coding using an adaptive morphological subband decomposition," *Proc. IEEE*, vol. 83, pp. 272–287, 1995.

[7] D. A. F. Florêncio, "A new sampling theory and a framework for nonlinear filter banks," Ph.D. dissertation, School Elect. Eng., Georgia Inst. Technol., Atlanta, 1996.

[8] F. J. Hampson and J.-C. Pesquet, "A nonlinear subband decomposition with perfect reconstruction," in *Proc. IEEE Int. Conf. Acoustics, Speech, Signal Processing*, Atlanta, GA, May 7–10, 1996, pp. 1523–1526.

[9] H. Cha and L. F. Chaparro, "Adaptive morphological representation of signals: Polynomial and wavelet methods," *Multidimen. Syst. Signal Process.*, vol. 8, pp. 249–271, 1997.

[10] R. Claypoole, G. Davis, W. Sweldens, and R. Baraniuk, "Nonlinear wavelet transforms for image coding," *Proc. 31st Asilomar Conf. Signals, Systems, Computers*, vol. 1, pp. 662–667, 1997.

[11] F. J. Hampson, "Méthodes non linéaires en codage d'images et estimation de mouvement," Ph.D. dissertation, Univ. Paris XI Orsay, Paris, France, 1997.

[12] R. L. Claypoole, R. G. Baraniuk, and R. D. Nowak, "Adaptive wavelet transforms via lifting," in *Proc. IEEE Int. Conf. Acoustics, Speech, Signal Processing*, Seattle, WA, May 12–15, 1998.

[13] ——, "Lifting construction of nonlinear wavelet transforms," in *Proc. IEEE-SP Int. Symp. Time-Frequency Time-Scale Analysis*, Pittsburgh, PA, Oct. 6–9, 1998, pp. 49–52.

[14] P. L. Combettes and J.-C. Pesquet, "Convex multiresolution analysis," *IEEE Trans. Pattern Anal. Machine Intell.*, vol. 20, pp. 1308–1318, 1998.

[15] J. Goutsias and H. J. A. M. Heijmans, "An axiomatic approach to multiresolution signal decomposition," in *Proc. IEEE Int. Conf. Image Processing*, Chicago, IL, Oct. 4–7, 1998.

[16] ——, "Multiresolution signal decomposition schemes—Part 1: Linear and morphological pyramids," CWI, Amsterdam, The Netherlands, Tech. Rep. PNA-R9810, Oct. 1998.

[17] F. J. Hampson and J.-C. Pesquet, "M-band nonlinear subband decompositions with perfect reconstruction," *IEEE Trans. Image Processing*, vol. 7, pp. 1547–1560, Nov. 1998.

[18] H. J. A. M. Heijmans and J. Goutsias, "Some thoughts on morphological pyramids and wavelets," in *Signal Processing IX: Theories and Applications*, S. Theodoridis, I. Pitas, A. Stouraitis, and N. Kaloupsidis, Eds. Rhodes, Greece: EUSIPCO, Sept. 8–11, 1998, pp. 133–136.

[19] ——, "Morphology-based perfect reconstruction filter banks," in *Proc. IEEE-SP Int. Symp. Time-Frequency Time-Scale Analysis*, Pittsburgh, PA, Oct. 6–9, 1998, pp. 353–356.

[20] B. Pouye, A. Benazza-Benyahia, I. Pollak, J.-C. Pesquet, and H. Krim, "Nonlinear frame-like decompositions," in *Signal Processing IX: Theories and Applications*, S. Theodoridis, I. Pitas, A. Stouraitis, and N. Kaloupsidis, Eds. Rhodes, Greece: EUSIPCO, Sept. 8–11, 1998, pp. 1393–1396.

[21] R. L. de Queiroz, D. A. F. Florêncio, and R. W. Schafer, "Nonexpansive pyramid for image coding using a nonlinear filterbank," *IEEE Trans. Image Processing*, vol. 7, pp. 246–252, Feb. 1998.

[22] R. L. Claypoole, R. G. Baraniuk, and R. D. Nowak, "Adaptive wavelet transforms via lifting," Dept. Elect. Comput. Eng., Rice Univ., Houston, TX, Tech. Rep. 9304, Apr. 1999.

[23] W. Sweldens, "The lifting scheme: A new philosophy in biorthogonal wavelet constructions," in *Proc. SPIE Wavelet Applications Signal Image Processing III*, vol. 2569, A. F. Lain and M. Unser, Eds., 1995, pp. 68–79.

[24] ——, "The lifting scheme: A custom-design construction of biorthogonal wavelets," *Appl. Comput. Harmon. Anal.*, vol. 3, pp. 186–200, 1996.

[25] ——, "The lifting scheme: A construction of second generation wavelets," *SIAM J. Math. Anal.*, vol. 29, pp. 511–546, 1998.

[26] F. A. M. L. Bruekers and A. W. M. van den Enden, "New networks for perfect inversion and perfect reconstruction," *IEEE J. Select. Areas Commun.*, vol. 10, pp. 130–137, 1992.

[27] H. J. A. M. Heijmans and J. Goutsias, "Constructing morphological wavelets with the lifting scheme," in *Pattern Recognition Information Processing, Proc. 5th Int. Conf. Pattern Recognition Information Processing (PRIP'99)*, Minsk, Belarus, May 18–20, 1999, pp. 65–72.

[28] S.-C. Pei and F.-C. Chen, "Subband decomposition of monochrome and color images by mathematical morphology," *Opt. Eng.*, vol. 30, pp. 921–933, 1991.

[29] ——, "Hierarchical image representation by mathematical morphology subband decomposition," *Pattern Recognit. Lett.*, vol. 16, pp. 183–192, 1995.

[30] S. Mallat, *A Wavelet Tour of Signal Processing*. San Diego, CA: Academic, 1998.

[31] H. J. A. M. Heijmans and J. Goutsias, "Multiresolution signal decomposition schemes—Part 2: Morphological wavelets," CWI, Amsterdam, The Netherlands, Tech. Rep. PNA-R9905, July 1999.

[32] M. Vetterli and J. Kovačević, *Wavelets and Subband Coding*. Englewood Cliffs, NJ: Prentice-Hall, 1995.

[33] S. Rănganath and H. Blume, "Hierarchical image decomposition and filtering using the S-transform," *Proc. SPIE Workshop Medical Imaging II*, vol. 914, pp. 799–814, 1988.

[34] A. Said and W. A. Pearlman, "An image multiresolution representation for lossless and lossy compression," *IEEE Trans. Image Processing*, vol. 5, pp. 1303–1310, 1996.

[35] J. Serra, *Image Analysis and Mathematical Morphology*. London, U.K.: Academic Press, 1982.
[36] H. J. A. M. Heijmans, *Morphological Image Operators*. Boston, MA: Academic, 1994.
[37] A. R. Calderbank, I. Daubechies, W. Sweldens, and B.-L. Yeo, "Wavelet transforms that map integers to integers," *Appl. Comput. Harmon. Anal.*, vol. 5, pp. 332–369, 1998.
[38] I. Daubechies and W. Sweldens, "Factoring wavelet transforms into lifting steps," *J. Fourier Anal. Applicat.*, vol. 4, pp. 245–267, 1998.
[39] D. L. Donoho, "De-noising by shoft-thresholding," *IEEE Trans. Inform. Theory*, vol. 41, pp. 613–627, 1995.
[40] M. D. Swanson and A. H. Tewfik, "A binary wavelet decomposition of binary images," *IEEE Trans. Image Processing*, vol. 5, pp. 1637–1650, Dec. 1996.
[41] R. Chellappa, C. L. Wilson, and S. Sirohey, "Human and machine recognition of faces: A survey," *Proc. IEEE*, vol. 83, pp. 705–740, 1995.
[42] L. Alvarez and J. M. Morel, "Formalization and computational aspects of image analysis," *Acta Numer.*, pp. 1–59, 1994.
[43] R. W. Brockett and P. Maragos, "Evolution equations for continuous-scale morphological filtering," *IEEE Trans. Signal Processing*, vol. 42, pp. 3377–3386, 1994.
[44] P. T. Jackway and M. Deriche, "Scale-space properties of the multiscale morphological dilation-erosion," *IEEE Trans. Pattern Anal. Machine Intell.*, vol. 18, pp. 38–51, Jan. 1996.
[45] R. van den Boomgaard and A. Smeulders, "The morphological structure of images: The differential equations of morphological scale-space," *IEEE Trans. Pattern Anal. Machine Intell.*, vol. 16, pp. 1101–1113, 1994.
[46] J. Weickert, *Anisotropic Diffusion in Image Processing*. Stuttgart, Germany: Teubner-Verlag, 1998.

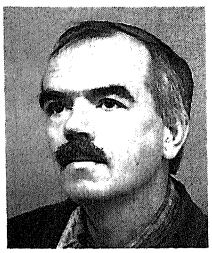

Henk J. A. M. Heijmans (M'97) received the M.S. degree in mathematics from the Technical University of Eindhoven, Eindhoven, The Netherlands, in 1981 and the Ph.D. degree from the University of Amsterdam, Amsterdam, The Netherlands, in 1985.

He joined the Center for Mathematics and Computer Science (CWI), Amsterdam, where he worked on mathematical biology, dynamical systems theory, and functional analysis. Currently, he is heading the research theme "signals and images" at CWI. His primary research interests concern the mathematical aspects of image processing and, in particular, mathematical morphology and wavelets.

John Goutsias (S'78–M'86–SM'94) received the Diploma degree in electrical engineering from the National Technical University of Athens, Athens, Greece, in 1981, and the M.S. and Ph.D. degrees in electrical engineering from the University of Southern California, Los Angeles, in 1982 and 1986, respectively.

In 1986, he joined the Department of Electrical and Computer Engineering, The Johns Hopkins University, Baltimore, MD, where he is currently a Professor. His research interests include one-dimensional and multi-dimensional digital signal processing, image processing and analysis, and mathematical morphology. He is currently an area editor for the *Journal of Visual Communication and Image Representation* and a Co-Editor for the *Journal of Mathematical Imaging and Vision*.

Dr. Goutsias served as an Associate Editor for the IEEE TRANSACTIONS ON SIGNAL PPROCESSING (1991–1993) and the IEEE TRANSACTIONS ON IMAGE PPROCESSING (1995–1997). He is a member of the Technical Chamber of Greece and Eta Kappa Nu, and a registered Professional Electronics Engineer in Greece.